GEOLOGICA CARPATHICA, 2024, 75, 1, 61–80 https://doi.org/10.31577/GeolCarp.2024.04

Inversion of deep-seated tectonics in the Central Depression of the Outer Carpathians (SE Poland)

JAN KUŚMIEREK[1], URSZULA BARAN[2] and GRZEGORZ MACHOWSKI[1,✉]

[1]AGH University of Krakow, Faculty of Geology, Geophysics and Environmental Protection, al. Mickiewicza 30, 30-059 Kraków, Poland
[2]Polish Oil and Gas Company, ul. M. Kasprzaka 25, 01-224 Warszawa, Poland

(Manuscript received October 8, 2023; accepted in revised form March 28, 2024; Associate Editor: Miroslav Bielik)

Abstract: The deeply buried, northeastern segment of the fold-and-thrust belt of the Outer Carpathians is contoured by synorogenic sediments (Upper Oligocene–Lower Miocene) of tectonically multiplied thicknesses, which mask the deep-seated structures. Integration of archival mappings and profiles of deep wells with the new generation of geological-seismic cross-sections reveals the unconformable position of asymmetric folds and duplexes built of synorogenic sediments, resting upon the older flysch formations (Cretaceous–Lower Paleogene). These structures are cut by a system of dislocated, monovergent, imbricated overthrusts, deeply rooted in the outer zones of thrust folds. These zones are associated with deep-seated, high-amplitude (up to several kilometres), Meso–Paleozoic and Precambrian faults originated by subduction of the European Platform. As revealed by geological reinterpretation of MT-1 magnetotelluric soundings, the time/space identification of longitudinal, compressional sutures rotated by transversal, transpressional faults suggests a segmented model of subduction of the platform basement. Its coincidence with the reconstructed kinematic evolution of sedimentary covers justifies the origin of the inversion tectonics of the Central Depression of the Outer Carpathians as a result of the heterogenic structure of the consolidated basement.

Keywords: fold-and-thrust belt, synorogenic sediments, consolidated basement tectonics of synclinoria, deep cross-sections, kinematic models

Introduction

The study area (Fig. 1) is bordered from the south by the Slovak part of the Carpathians and from the east by the Ukrainian part of the Carpathians. This area comprises outcrops of thrust folds belonging to the so-called Middle Group (Nowak 1927), which constitutes the eastern part of the Polish Carpathians. The oil-bearing synclinoria of these thrust folds are associated with the hybrid depression of the consolidated basement known as the Central Depression of the Outer Carpathians (CDOC; Tołwiński 1932). This structure extends eastward to the Ukrainian Carpathians, where it is named the Krosno Zone (Kolodij et al. 2004). Its northwestern border is the Muszyna–Jasło (M-J) dislocation, which relocates the structural elements of the deep basement (Fig. 1).

The detailed structural and facies studies in this area were triggered by discoveries of shallow oil deposits at the turn of the 19th and 20th centuries. Recently, the exploration targets have been deep-seated hydrocarbon traps and unconventional hydrocarbon deposits. However, crucial to the recognition of deep-seated synclinoria in the CDOC was the application of a modified methodology of seismic survey by the Geophysical Co. in Kraków after 1994 (Czerwińska 2013). Integration of modern seismic imagery with profiles of deep wells supported by detailed mapping of intersections of folds and overthrusts revealed the disharmonic tectonic style of synorogenic sediments in relation to the older flysch formations detached from the top surface of the consolidated basement.

The authors aim to present selected examples of inversion tectonics of synclinoria and to relate their origin to detailed models of the top of the consolidated basement. The basis is the geological interpretation of hundreds of magnetotelluric soundings carried out by the PBG Geophysical Exploration Ltd. in Warsaw, in the years 1997–2003, using the new MT-1 recording and interpretation system (for details, see Czerwiński & Stefaniuk 2005; Stefaniuk et al. 2009).

The results of the geological interpretation of new geophysical surveys document a much more complicated, deep tectonic structure of the CDOC (Kuśmierek 2010; Kuśmierek et al. 2010, 2016, 2019; Kuśmierek & Baran 2016) in comparison with the cross-sections previously published by other authors (e.g., Wdowiarz 1985; Klecker et al. 2001; Oszczypko 2004; Nemčok & Henk 2006; Nemčok et al. 2006; Oszczypko et al. 2008; Gągała et al. 2012).

Outline of fold-and-thrust tectonics of the study area

Significant diversity of tectonic styles of geological structures observed in the northern segment of the Carpathians is revealed by discrepancy of nappes belonging to the Magura Nappe, the Middle (Dukla Nappe, Silesian Nappe, Subsilesian

✉ corresponding author: Grzegorz Machowski
machog@agh.edu.pl

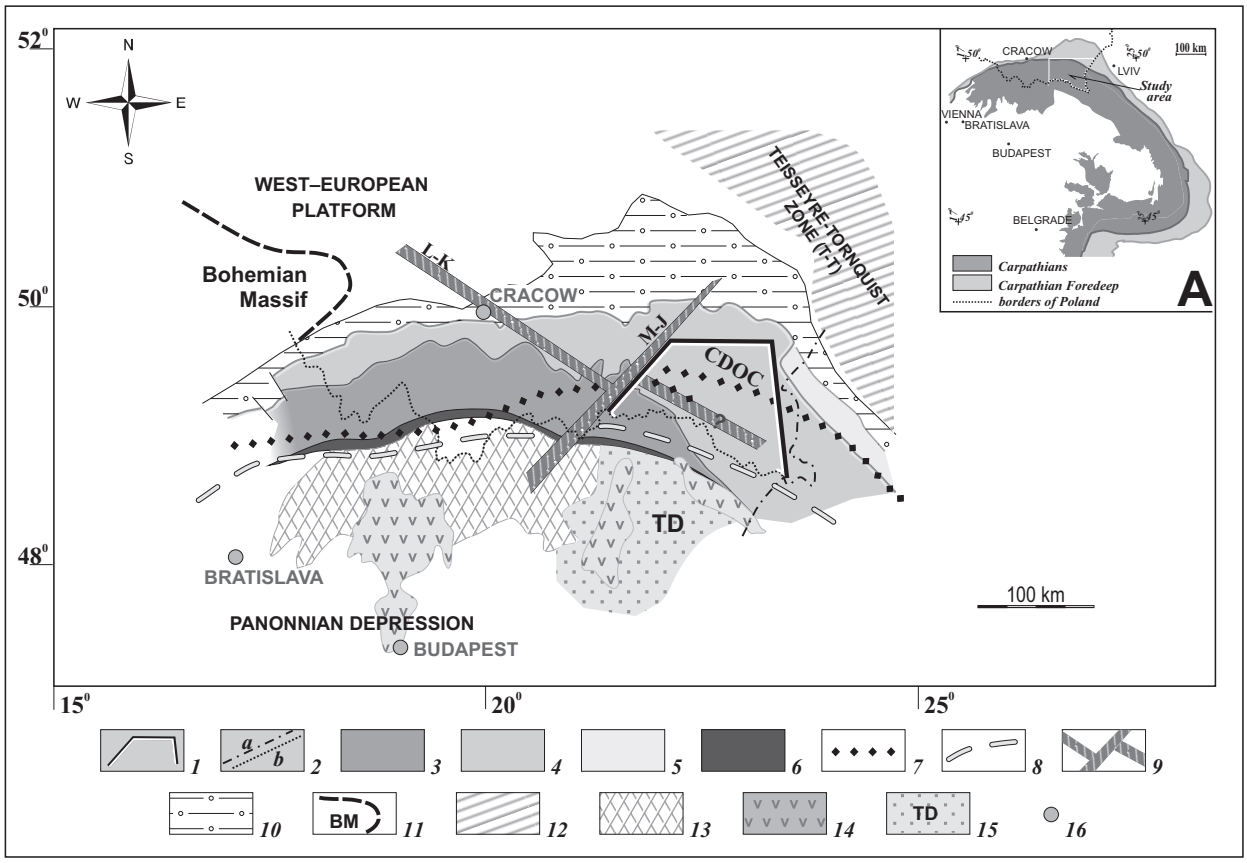

Fig. 1. Northeastern segment of the Carpathian arc and its geostructural frames: **A** – location of study area within the Carpathian arc. Legend: 1 – range of new interpretation of the western part of Central Depression of the Outer Carpathians (CDOC); 2 – western boundary of the Ukrainian Carpathians (a) and the northern boundary of the Slovak Carpathians (b). Groups of Outer Carpathian nappes: 3 – Magura Nappe; 4 – Dukla Nappe, Silesian Nappe, Subsilesian Unit, and Skole Nappe; 5 – Boryslav–Pokuttya Unit, Stebnik Unit, and Zgłobice Unit); 6 – Pieniny Klippen Belt; 7 – axes of gravity minimum (after Woźnicki 1985); 8 – zone of 0-values of geomagnetic induction vector (after Jankowski et al. 1979); 9 – major deep-seated dislocations (deep fractures) in the basement of the Eastern Polish Carpathians: L-K – Lubliniec-Kraków, M-J – Muszyna–Jasło, 10 – Carpathian Foredeep, 11 – Bohemian Massif (BM), 12 – Teisseyre–Tornquist Zone (T-T), 13 – Inner Western Carpathians (Slovak Block), 14 – Neogene volcanic covers, 15 – Transcarpathian Depression (TD), 16 – cities.

Unit, and Skole Nappe), and the Marginal (Boryslav–Pokuttya, Stebnik, and Zgłobice units) groups, demonstrated by non-continuous intersection of the axis of regional gravity minimum and 0-values of geomagnetic induction vector (Fig. 1).

The structural position of oil-bearing synclinoria within the CDOC is determined from a wide belt of outcrops of the youngest synorogenic sediments (Upper Oligocene–Lower Miocene) of synkinematic type (McClay 2011) known as the Menilite-Krosno Series (MKS; Jucha & Kotlarczyk 1958). These folded sediments infill the two synclinoria of the Middle Group of nappes: the Silesian Synclinorium (known also as the Central Synclinorium, Świdziński 1958) and the Skole Synclinorium. Both structures are separated by the outcrops of the Subsilesian Nappe contoured by its overthrust, which extends as far as the border zone with the Ukrainian Carpathians (Fig. 2).

Depocenters of the MKS are associated with the outer zones of the synclinoria (Fig. 3): the Skole Synclinorium located east of the Wisłok River valley and the Silesian Synclinorium extending as far as to the Wisłoka River Basin (Fig. 2). These zones reveal exceptionally complicated tectonics of sedimentary covers and their basement (Figs. 4, 5).

Maximum thicknesses of MKS in the Silesian Synclinorium coincide with the area of morphological depression named the Jasło–Sanok Depression, which constitutes the foreland of the Dukla Nappe overthrust (Kozikowski 1958; Wdowiarz 1985). In this area, the diachronous deposition of lithofacies members belonging to the MKS, in relation to the regional stratigraphic marker horizon of the thin-bedded Jasło Limestone (of characteristic shaly parting, Jucha 1969), is illustrated by the chronostratigraphic model (Fig. 3A).

The diverse tectonic style of the Silesian Synclinorium is best visible in the Muszyna–Jasło Fault Zone (M-J; Fig. 1), which separates the CDOC from the Gorlice Depression located in its southwestern extension. The structure of M-J is illustrated by the western cross-section (Fig. 4). Here, the outcrops of the MKS are segmented by strongly-uplifted synsedimentary folds. In their culmination, the older formations are

exposed, deeply dissected by synkinematic erosion (Świderski 1933; Kuśmierek 1990). In that cross-section, the internal zone of the Silesian Synclinorium is covered by tectonic-erosional lobes of the Magura Nappe or its locally isolated, smaller tectonic sheets (Świdziński 1971). According to other concepts (Żelaźniewicz et al. 2011), these sheets belong to the so-called Jasło Subnappe formed at the front of the Magura Nappe.

The northern part of that cross-section documents the tectonics of the uplifted part of the Skole Nappe thrust at a low angle over the slope of the Carpathian Foredeep. Here, MKS sediments are generally absent. Profiles of deep wells demonstrate the monovergent system of geometrically complicated thrusts, which control the amount of tectonic reduction of covering nappes and which are in contrast with the block-type tectonic style of the basement. The basement is dominated by high-angle faults that disappear in the top parts of the Miocene autochthonous molasse formation. The Miocene formation pinches out on the slope of the platform (Kuśmierek & Baran 2016).

The eastern cross-section (Fig. 5), which is positioned in the border zone with the Ukrainian Carpathians, shows extremely

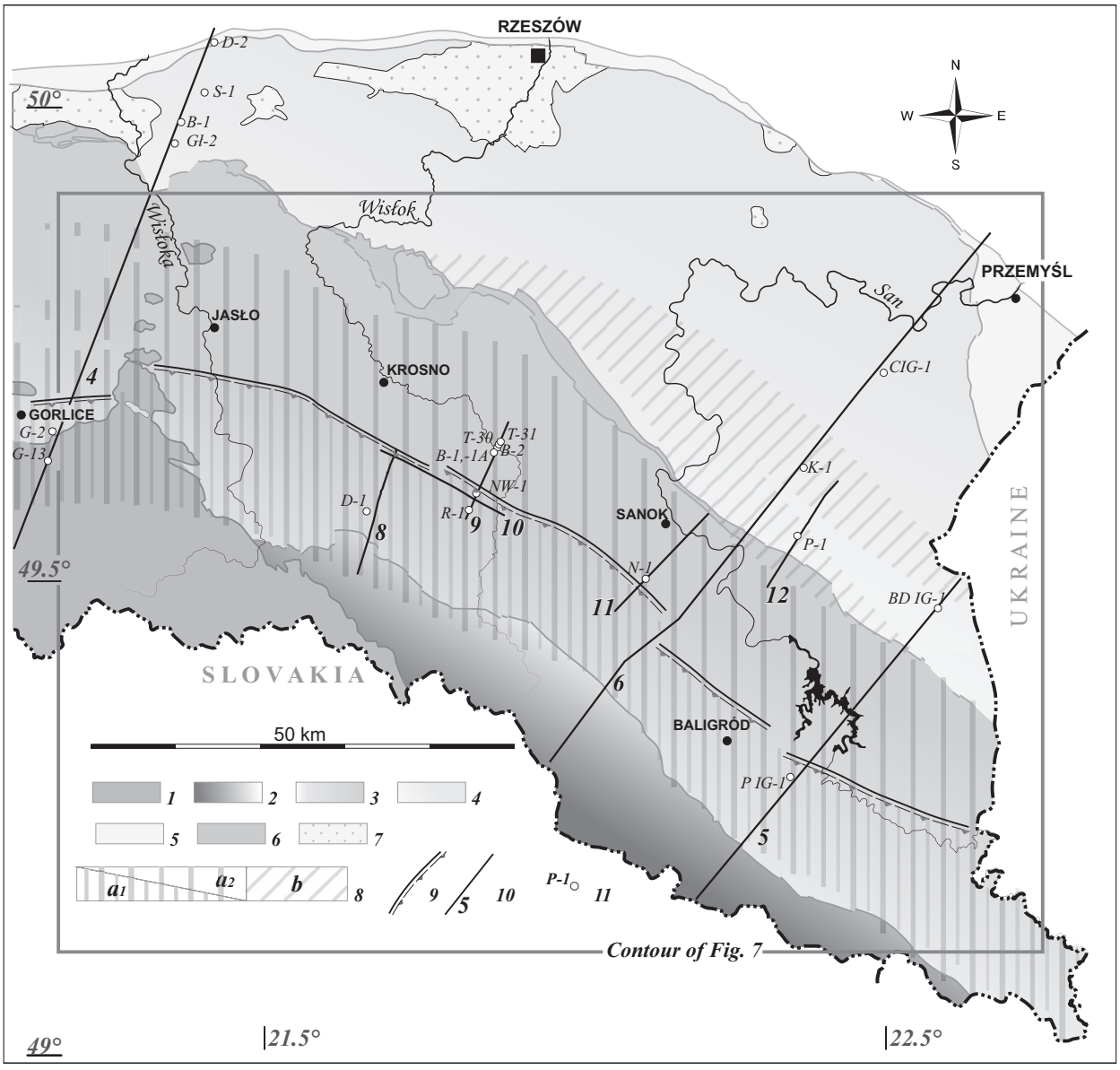

Fig. 2. Structural sketch-map of the Polish Eastern Carpathians. Nappes (1–5): 1 – Magura; 2 – Dukla; 3 – Silesian; 4 – Skole; 5 – Boryslav–Pokuttya Unit, Stebnik Unit, and Zgłobice Unit; 6 – outcrops of Subsilesian Unit; 7 – large sheets of transgressive Miocene formation unconformably resting upon the flysch; 8 – depocenters of synorogenic sediments (Oligocene–Lower Miocene) contoured by isohypse of initial stratigraphic thickness >1600 m within: a – Silesian Nappe (a_1 – inner part, a_2 – outer part), b – Skole Nappe; 9 – overthrust of the inner (southern) zone of Silesian Nappe (I/O); 10 – location of the cross-sections in Figs. 4–6 and 8–12 and the model of Precambrian top surface (Fig. 7); 11 – location of deep wells shown in Figs. 4–12.

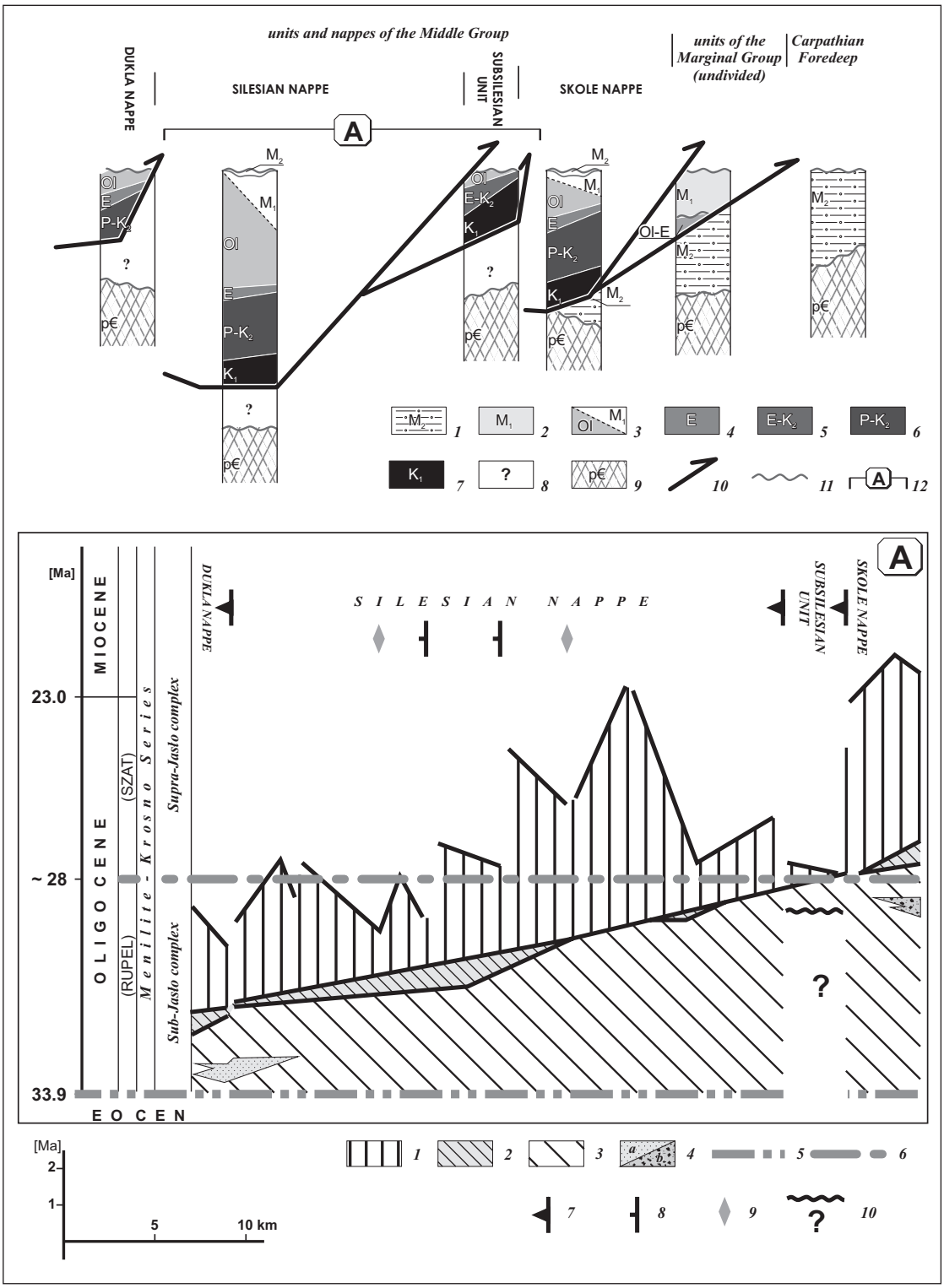

Fig. 3. Synthetic stratigraphic columns of nappes, tectonic-facies units and their basement in the Polish Eastern Carpathians (from Kuśmierek 2010, detailed). Sedimentary cover: 1 – autochthonous molasses of Carpathian Foredeep and their paraautochthonous erosional sheets unconformably covering the nappes; 2 – folded molasses of the Marginal Group; 3 – Menilite-Krosno Series (synorogenic sediments). Older sedimentary formations: 4 – Eocene; 5 – Upper Cretaceous, Paleocene and Eocene (undivided); 6 – Upper Cretaceous–Paleocene; 7 – Lower Cretaceous. Consolidated basement: 8 – unidentified Meso–Paleozoic formations; 9 – Precambrian (Eocambrian); 10 – nappes overthrusts; 11 – erosional-sedimentary unconformities; 12 – range of Fig. 3A. **A** – Chronostratigraphic model of synorogenic sediments of the Menilite-Krosno Series in the Jasło–Sanok area: 1 – Krosno lithofacies; 2 – Transitional Beds; 3 – Menilite lithofacies; 4 – intra-Menilite sandstones: *a* – Cergowa type, *b* – Kliwa type; 5 – Jasło Limestones (oldest horizon); 6 – Globigerina Marls; 7 – nappes overthrusts; 8 – synsedimentary folds overthrusts; 9 – axes of synsedimentary anticlines; 10 – synsedimentary gap in the Subsilesian Unit (from Jucha 1969).

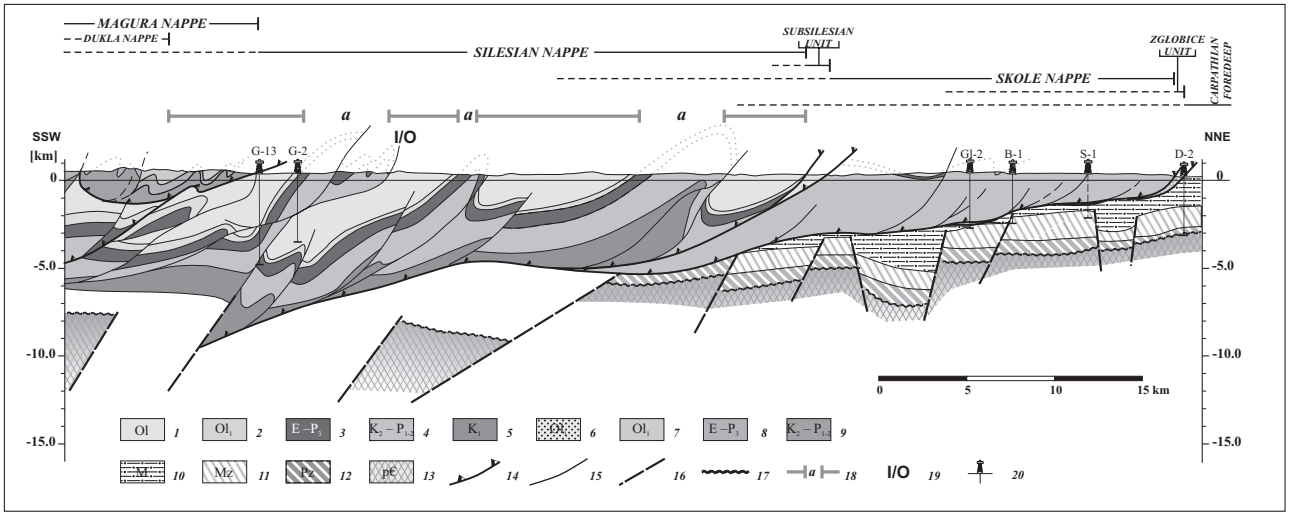

Fig. 4. Western cross-section Uście Gorlickie–Pustków (from Kuśmierek & Baran 2013). Nappes and units of the Middle Group: 1– Krosno Beds (undivided); 2 – Transitional and Menilite beds (undivided); 3 – Hieroglyphic Beds, Variegated shales, and Ciężkowice Sandstone; 4 – Inoceramus, Istebna, and Godula beds (undivided); 5 – Lgota, Wierzowa, and Cieszyn beds (undivided); 6 – folded Miocene. Magura Nappe: 7 – Lower Oligocene; 8 – Upper Paleocene–Eocene; 9 – Upper Cretaceous–Lower Paleocene. Autochthonous series: 10 – Upper Miocene (Badenian–Sarmatian); 11 – Mesozoic; 12 – Paleozoic; 13 – Precambrian; 14 – overthrust nappes; 15 – folds overthrusts and duplexes; 16 – basement faults (deep discontinuities); 17 – top of Precambrian; 18 – range of CDOC: *a* – culminations of synsedimentary folds; 19 – I/O – thrust of inner (southern) zone of Silesian Synclinorium over its outer zone; 20 – deep wells.

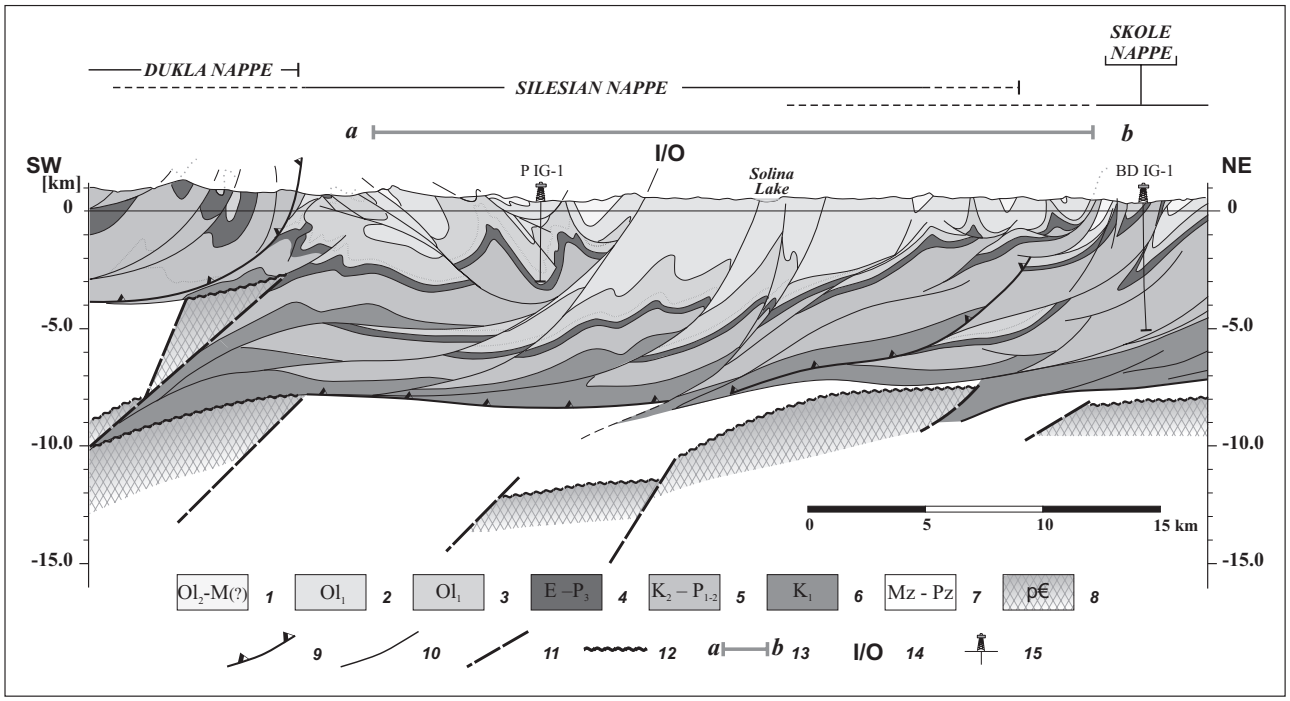

Fig. 5. Eastern cross-section – Cisna–Dobromil (from Kuśmierek & Baran 2013). Nappes and units of the Middle Group: 1– Middle and Upper Krosno Beds (undivided); 2 – Lower Krosno Beds; 3 – Transitional and Menilite beds (undivided); 4 – Hieroglyphic Beds, Variegated shales, and Ciężkowice Sandstone; 5 – Łupków, Cisna, Istebna, and Inoceramus beds (undivided); 6 – Lgota, Spas, Wierzowa, and Cieszyn beds (undivided). Autochthonous Series: 7 – unidentified Meso–Paleozoic sediments; 8 – Precambrian; 9 – overthrust nappes; 10 – fold overthrusts and duplexes; 11 – basement faults (deep fractures); 12 – top of Precambrian; 13 – range of CDOC, interfingering zones of Silesian facies with *a* – Dukla facies and *b* – Skole facies; 14 – I/O – the thrust of the inner (southern) zone of the Silesian Synclinorium over its outer zone; 15 – deep wells.

complicated tectonics of both the sedimentary cover and its basement. Detailed field observations run in the foreland of the Dukla Nappe and demonstrate the presence of backthrusts of a southwestern vergence, which displace the limbs of synsedimentary folds. This causes drastic changes in the thickness of thick-bedded Krosno Sandstone (Kuśmierek 1979, 1981).

The tectonic style of the northern part of the cross-section is characterized by a consequent system of deep-seated, southeast-dipping thrusts associated with the increasing depth toward the bottom of the MKS along the I/O overthrust (Fig. 5). Within the border zone of the Skole Synclinorium, outcrops of the MKS are segmented by disharmonic anticlinal uplifts. Complicated tectonics of Upper Cretaceous–Lower Paleogene formations in these uplifts is revealed by deep wells (e.g., BD IG-1, Żytko 2006).

Data from deep wells (e.g., G-2 and G-13, Fig. 4) indicate that the inversion style of tectonic structure of older flysch formations is typical of the inner zones of synclinoria, particularly where the thick-bedded Ciężkowice and Istebna sandstones pinch out.

Magnetotelluric tectonic models of consolidated basement

Modified geological interpretation of the tectonic structure of the consolidated basement was applied to the tectonic depressions of the CDOC and to the fragment of the platform slope, which borders the CDOC from the northeast. (Figs. 6, 7). The western border of these depressions is the northern extension of the Muráň Fault (Maheľ 1974), which extends beneath the Carpathian Foredeep and is known as the Muszyna–Jasło Fault Zone (M-J, Fig. 1; Doktór et al. 1990). This dislocation displaces to the southwest the axes of a gravity minimum (Woźnicki 1985), the 0-values of the geomagnetic induction vector (Jankowski et al. 1984), and a trace of the subvertical Lubliniec–Kraków Fracture Zone (L-K, Fig. 1). The latter structure separates the Małopolska and Silesian basement blocks (Żelaźniewicz et al. 2011).

A major breakthrough in mapping the morphology of the consolidated basement was a preliminary interpretation of five magnetotelluric sounding traverses (E-1, E-2, E-3, E-4, and F-1) completed in the study area in the years 1975–1990 (for details, see e.g., Święcicka-Pawliszyn & Pawliszyn 1978; Stefaniuk & Kuśmierek 1986; Doktór et al. 1990; Kuśmierek 1990, 1996; Ryłko & Tomaś 1995; Stefaniuk 2003). The results documented a non-continuous geometry of the top surface of the consolidated basement dissected by deep-seated faults of significant throws. However, these dislocations remained undisclosed by refraction seismics. Precise information about resistivity distribution down to 25 km depth (including the sedimentary cover) was provided by the Electromagnetic Instruments MT-1 System of frequency recording range extended to about 500 Hz (for details, see Stefaniuk 2003; Czerwiński & Stefaniuk 2005).

The shallower parts of geoelectric cross-sections identified as the images of allochthonous nappes sheets are characterized by oblique (vergent) geometry of resistivity boundaries (within the range of low and medium resistivity values). These are different from images of flat-lying Miocene molasses resting upon the high-resistivity Precambrian basement on the slope of the platform (Stefaniuk 2003). Implementation of the MT-1 system enabled the researchers to apply the advanced data processing methodology leading to the generation of 1D and 2D inversion models.

Especially useful was, among others, the 2D NLCG algorithm, designed to contour the geometry of high-angle resistivity boundaries under the conditions of extreme resistivity contrasts, typical of the consolidated basement of the CDOC (Stefaniuk et al. 2009). It should be emphasized that a more advanced interpretation, i.e. 3D, often performed in the Polish Lowlands (e.g., Ślęzak et al. 2016; Oryński et al. 2022) in the tectonically complex CDOC area would be difficult to implement.

The results of the geological interpretation of the Radoszyce–Przemyśl geoelectric cross-section processed with the 2D NLCG algorithm are shown in Fig. 6 (from Kuśmierek et al. 2019). This cross-section includes the benchmark profiles of deep wells (C IG-1 and K-1), which penetrated the erosional-tectonic elevation of the platform slope and demonstrates its different tectonic structure, in comparison with deeply buried depressions of the CDOC.

The principal reinterpretation target of magnetotelluric soundings was geological identification of the traces of deep-seated faults combined with recognition of their geometric parameters: dimensions and directions of tectonic movements in planes of geoelectric cross-sections. Extreme diversity of rock resistivity (from several to over 1000 Ω·m) together with complicated geometry of resistivity boundaries justified the distinction of three-time/space generations of discontinuities: (i) erosional-tectonic, of flat geometry, (ii) longitudinal, high-angle faults of maximum amplitudes operating as younger compressional sutures of the basement, and (iii) transversal or oblique, sub-vertical, oblique-slip deep dislocations inherited after the stage of expansion of sedimentary basins and rejuvenated in the Neogene. The latter contoured the rebuilding of the heterogenic tectonic structure of the CDOC.

White fields visible in Fig. 7 mark the areas for which interpretation of basement morphology within the tectonic blocks could not be credibly done due to the lack of transversal geoelectric cross-sections. The exception is the No. 24 longitudinal cross-section along which the burial depth of the Precambrian top surface locally falls below the depth range of interpretable resistivity of the rocks (i.e., about 25 km b.s.l., Stefaniuk 2003).

The time/space correlation of selected generations of deep-seated faults played a key role in generation of a hypsometric model of the Precambrian basement (Fig. 7). In the northern part of the study area, reinterpretation of magnetotelluric soundings was integrated with the results of seismic surveys and deep drillings penetrating the Precambrian basement

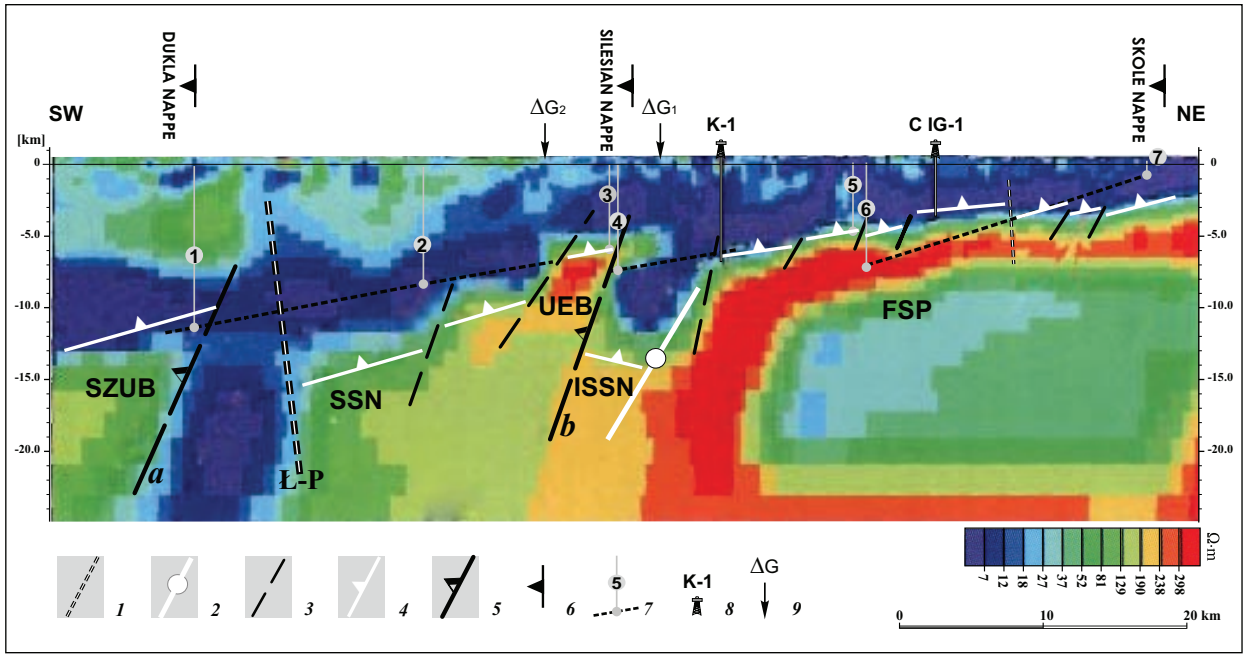

Fig. 6. Geological reinterpretation of the basement model with reference to the results of inversion of 2D NLCG magnetotelluric soundings along the No. 16 Radoszyce–Przemyśl profile (from Stefaniuk et al. 2009). 1 – Subvertical, oblique-slip faults (deep fractures) transversal to CDOC strike (among others: Łupków–Przemyśl, Ł-P); 2 – longitudinal deep fracture contouring the range of the platform slope; 3 – longitudinal, subvertical basement faults; 4 – shallow compressional sutures of flat geometry; 5 – deep, compressional sutures of throws >5 km contouring inner zones of synclinoria: *a* – Silesian, *b* – Skole; 6 – an intersection of overthrust nappes; 7 – depths to the top of the consolidated basement before deposition of synorogenic sediments (h_1–h_7, hypothetical interpolation); 8 – wells penetrating top of Precambrian; 9 – ΔG_1, ΔG_2 – axes of regional gravity minimum. SZUB – the southern zone of the uplifted basement; SSN – synclinorium of the Silesian Nappe; UEB – uplifted element of basement identified as Subsilesian Unit; ISSW – inner synclinorium of the Skole Nappe; FSP – flexural slope of the platform.

(for details, see e.g., Kuśmierek & Baran 2008, 2016; Baran & Jawor 2009). In that area, extreme resistivity values of the basement contrasted with low values of flat-lying autochthonous Miocene sediments, which covered the erosional-tectonic morphology of the basement surface along the low-angle platform slope (Fig. 4). The deepest penetration of the platform slope by the K-1 well (Fig. 7) revealed radically different features of the geoelectric cross-section in comparison with that of the remobilized basement of the CDOC (Fig. 6). Its northern range was contoured by the outer, Type 2 compressional suture of a multi-kilometre amplitude. Its intersection, dislocated by transversal fractures, is illustrated in Fig. 7.

According to the 2D inversion model, a cross-section through the CDOC demonstrates the presence of an upper hypsometric level (having vergent resistivity boundaries), which illustrates the tectonics of the nappes. The level is contoured by a flat-lying discontinuity identified as the Type 1 compressional suture, which, in turn, is cut by the sub-vertical Type 2 faults dipping to the southwest. Among them are tectonic sutures (a and b) related to the inner edges of the Silesian and the Skole synclinoria (Fig. 6). It is suggested that the low-resistivity (about several Ω·m) sediment formation accompanying the edge "a", similarly to the zone of 0-values of the geomagnetic induction vector (Fig. 1), may be related to the subduction process (Woźnicki 1985).

This suggestion is supported by an exceptionally complicated model of the top of the Precambrian basement (Fig. 7), which shows a mosaic of blocks of very diverse hypsometry, typical of buried zones of the platform. In the tectonic depressions of the CDOC, the top of the Precambrian basement is covered by a thick pile of Phanerozoic platform formations of unrecognized stratigraphy, which, unfortunately, occur below the depth range of deep wells. Hence, the structural models of the consolidated basement are limited exclusively to the identification of the geometry of deep-seated faults, important for the interpretation of the origin of the inversion tectonics of the CDOC sedimentary cover.

Seismic and geological reinterpretation of sedimentary cover tectonics

Reinterpretation criteria and procedure

The absence of regional reflection horizons, along with interference and low quality of seismic records acquired in the epoch before digital data recording methodology, resulted in skepticism among scientists concerning the usefulness of seismic imaging for the interpretation of deep tectonics of the Carpathian nappes (Wdowiarz 1985). The reason was, among

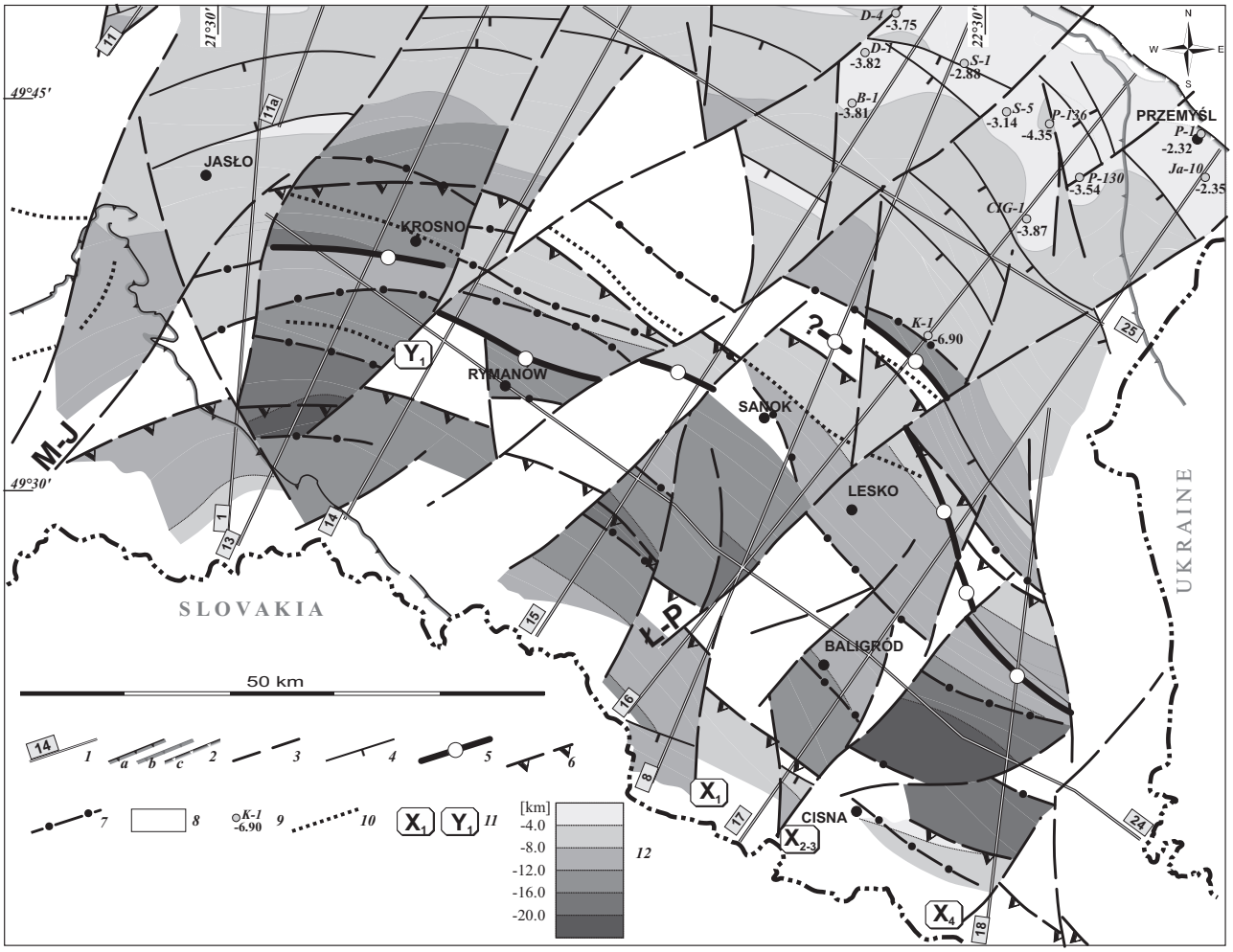

Fig. 7. Magnetotelluric structural model of the top of the Precambrian basement: 1 – location and symbol of the magnetotelluric profile; 2 – intersections of overthrust nappes of groups: *a* – Magura, *b* – Middle, *c* – Marginal; 3 – high-angle, oblique-slip faults (deep fractures), transversal and oblique to the CDOC strike. Platform slope: 4 – longitudinal, normal and reverse faults of amplitudes <3 km, with dip directions; 5 – longitudinal deep fracture of throw >6 km, which contours the range of flexural platform slope. The CDOC: 6 – deep compressional sutures, which contour the inner ranges of tectonic depressions of the Silesian and Skole synclinoria; 7 – longitudinal sub-vertical faults of throws >3 km; 8 – basement blocks of unidentified geometry. Symbols: 9 – wells with depths to the top of Precambrian [km b.s.l.]; 10 – axes of negative gravity anomalies; 11 – basement transversal faults, which modify tectonic style (Y_1 in the northwestern zone; X_1, X_{2-3} and X_4 in the southeastern zone); 12 – depth intervals of the Precambrian basement (related so sea level datum).

others, the unexplained, divergent dip angles of Oligocene versus Cretaceous–Eocene formations (Kuśmierek et al. 1985) confirmed in the subsequent years by the results of deep drillings (Fig. 2).

After 1994, the Geophysical Co. in Kraków implemented a modern methodology of seismic survey (Czerwińska 2013), particularly the advanced procedures of seismic data processing with the ProMAX system (for details, see e.g., Marecik et al. 2008) applied to a model of velocity fields and pre-stack depth migration (PSDM). This progress enabled the researchers to obtain an improved image of seismic boundaries (having better dynamics and resolution), especially of thick-bedded sandstone formations.

The presented reinterpretation examples of deep-seated tectonics of the CDOC synclinoria focused on the zones of extremely complicated geological structure (Figs. 8–12). These examples were selected from some tens of new geological and seismic cross-sections constructed by the authors in the years 2009–2016, during the completion of several hydrocarbon exploration projects. The projects aimed to evaluate the opportunities of new discoveries of: (i) hydrocarbon deposits in deep-seated traps, yet unexplored by drillings, and (ii) unconventional hydrocarbon accumulations (for details, see Kuśmierek et al. 2010, 2016, 2019).

The iterative procedure of geological reinterpretation included the following steps:

- generation of initial structural models using seismic time sections, including the identification of lithostratigraphic boundaries (less readable in deeper time sections, below 2.5–3.5 sec intervals) to estimate the velocity fields of

distinguished sedimentary complexes for depth migration (PSDM). It was supported by correlation with the trends of thickness changes within the CDOC synclinoria (from Kuśmierek et al. 1991–1994).

- construction of deep geological and seismic cross-sections, integrated in the near-surface zone with the interpretation of intersection patterns on detailed, uncovered geological maps. The maps were prepared by the Polish Geological Institute and updated by GeoKrak Ltd. (Starzec 2016). At greater depths, the traces of dislocations (thrusts, duplexes, and faults) and lithostratigraphic boundaries were referred to the final geometry of reprocessed seismic profiles (after depth migration) correlated with the profiles of deep wells (acquired from archival materials of the Polish Oil and Gas Co., Jasło Branch).

Silesian Synclinorium

The internal zone of the Silesian Synclinorium is marked with a special pattern in Fig. 2. The zone is contoured by the intersection line of the overthrust of the Targowiska–Besko–Mokre folds showing the maximum amplitude of tectonic transport and marked "I/O" on the Traverse cross-sections (Figs. 4, 5), as well as on geological-seismic cross-sections (Figs. 8–11). East of the transversal M-J fracture (Fig. 1), the intersection line of that thrust is displaced by numerous transversal faults developed in the basement of the Silesian Synclinorium (Fig. 7), which separate the thrust from the Gorlice Structural Depression (Figs. 2, 4).

The tectonic style of the western segment of the inner zone in the Silesian Synclinorium is illustrated by a fragment of transversal, geological-seismic cross-section (Fig. 8) correlated with the profile of the D-1 deep well. The well was positioned on the outcrop of the elevated Draganowa–Iwonicz Zdrój Fold, distinguished as the regional structural element A. The D-1 deep well, completed down to 5500 m final depth, encountered traces of three imbricated thrusts (or duplexes) displacing the northern limbs of the folds, and it is distinguished as structural elements of B, C, and D (Fig. 8). However, from these three elements, only the D element is revealed in the intersection of the surface geological map, unlike the overlays of A, B, and C elements. D element has an intersection line marked on the geological map (Starzec 2016), whereas the remaining A, B, and C elements fade in the near-surface zone. Within the outcrops of the Krosno lithofacies, amplitudes of these three structural elements are compensated by asymmetric folds (Fig. 8).

Considering the regional scale, the most complicated tectonic structure was encountered in the southern part of the Silesian Synclinorium, which builds the foreland of the Dukla

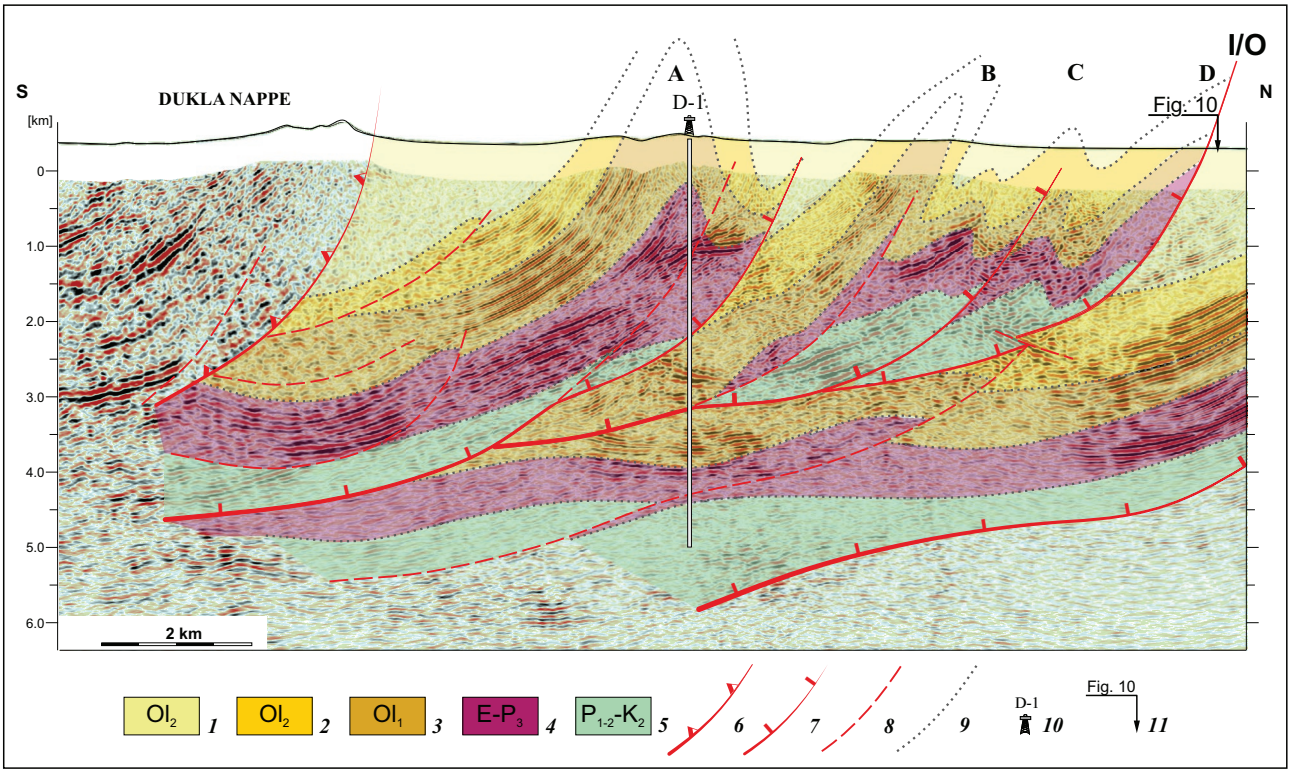

Fig. 8. Cross-section through the southwestern, inner zone of the Silesian Synclinorium (after Kuśmierek et al. 2019). Silesian Series: 1 – Upper Krosno Beds; 2 – Lower Krosno Beds; 3 – Menilite and Transitional beds (undivided); 4 – Hieroglyphic Beds, Variegated shales, and Ciężkowice Sandstone (undivided); 5 – Istebna Beds; 6 – overthrust nappes; 7 – fold overthrusts, I/O – the thrust of the inner (southern) zone of the Silesian Synclinorium over its outer zone; 8 – second-order duplexes (decollements) and faults; 9 – lithostratigraphic boundaries; 10 – well profile; 11 – location of longitudinal cross-section. A–D – distinguished structural elements.

Unit overthrust. It is observed on both the western cross-section (Fig. 4), which includes the Gorlice Depression and on the eastern cross-section (Fig. 5), southeast of Baligród, where the surface intersection image of the Draganowa–Iwonicz Zdrój Fold (structural element A) reveals overturned folds and backthrusts (Kuśmierek 1979, 2010). Moreover, the Zboj-1 deep well in Slovakia (about 15 km southwest from the Dukla Unit overthrust), penetrated the Upper Eocene–Oligocene succession at a depth interval of 3800–5002 m, beneath the Dukla Unit overthrust (Ďurkovič et al. 1982). That succession presumably represents the marginal zone of the Silesian Unit.

Attention must be paid to the geological-seismic cross-section shown in Fig. 9, which is perfectly documented by seven wells, including the R-1 and B-1A wells, with final depths exceeding 5000 m. This cross-section illustrates the tectonic structure of the Silesian Synclinorium at the interfingered contact of its inner and outer zones (Fig. 2) along the I/O overthrust. The amplitude of that overthrust decreases from about 5 km at the bottom of the Menilite Beds to 2 km in the near-surface zone.

In contrast to the inner zone of the Silesian Synclinorium, which is strongly dislocated by duplexes (as revealed by the upper segment of the R-1 deep well) in its outer zone, the extremely thick synorogenic sediments of the Krosno lithofacies build the open folds. However, beneath these folds, the deep-seated, flat-lying overthrusts are hidden, which displace the Early Oligocene–Eocene formations, as documented by the B-1A and B-2 deep wells. In the near-surface zone, the intersections of these overthrusts appear exclusively in the frontal, asymmetric anticlinal uplift (Fig. 9). Strong thickness reduction of the Krosno Beds in the northern limb of that anticline advocates the rejuvenation of these flat overthrusts during the deposition of younger, synorogenic sediments (Fig. 3A) that are combined with: (i) their redeposition towards the steep slopes of the Silesian Subbasin, (ii) the presence of scattered angular unconformities in the stratigraphic column, and (iii) probable submarine erosion (Książkiewicz 1956; Jucha 1969; Kuśmierek 1990).

A fragment of the longitudinal geological-seismic cross-section is shown in Fig. 10, which connects the transversal cross-sections seen in Figs. 8 and 9, demonstrating the difficulties in correlation with the distinguished structural elements at the interfingered contact between the inner and the outer zones of the Silesian Synclinorium. In comparison with the shallower part of that cross-section, which presents the geological image consistent with that shown on detailed geological maps (Starzec 2016), the deep-seated tectonic structure reconstructed from reprocessed seismic profiles presents numerous duplexes built of older, Cretaceous–Eocene sediments showing advanced diagenesis. The duplexes appear to be induced by transversal faults of various dip angles and amplitudes of displacement, which, in turn, were triggered by dislocations in the consolidated basement.

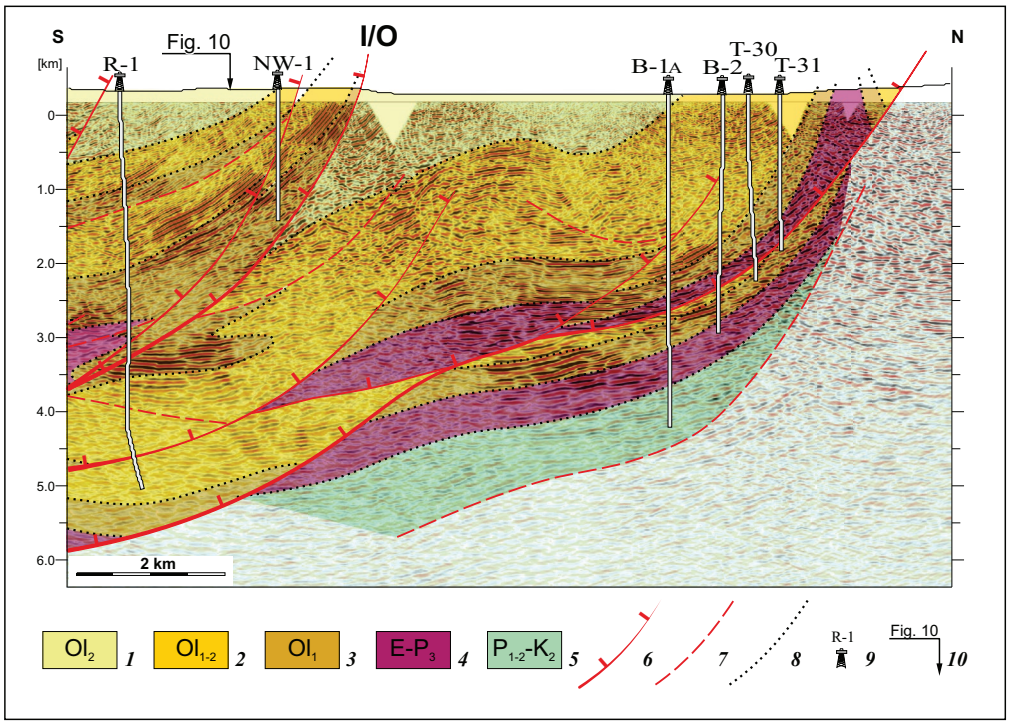

Fig. 9. Example of correlation of seismic cross-section through the central part of the Silesian Synclinorium with profiles of deep wells (from Kuśmierek et al. 2019, fragment). Silesian Series: 1 – Upper Krosno Beds; 2 – Lower Krosno Beds; 3 – Menilite and Transitional beds (undivided); 4 – Hieroglyphic Beds, Variegated shales, and Ciężkowice Sandstone (undivided); 5 – Istebna Beds; 6 – fold overthrusts, I/O – the thrust of the inner (southern) zone of the Silesian Synclinorium over its outer zone; 7 – second-order duplexes (decollements) and faults; 8 – lithostratigraphic boundaries; 9 – wells profiles; 10 – location of longitudinal cross-section.

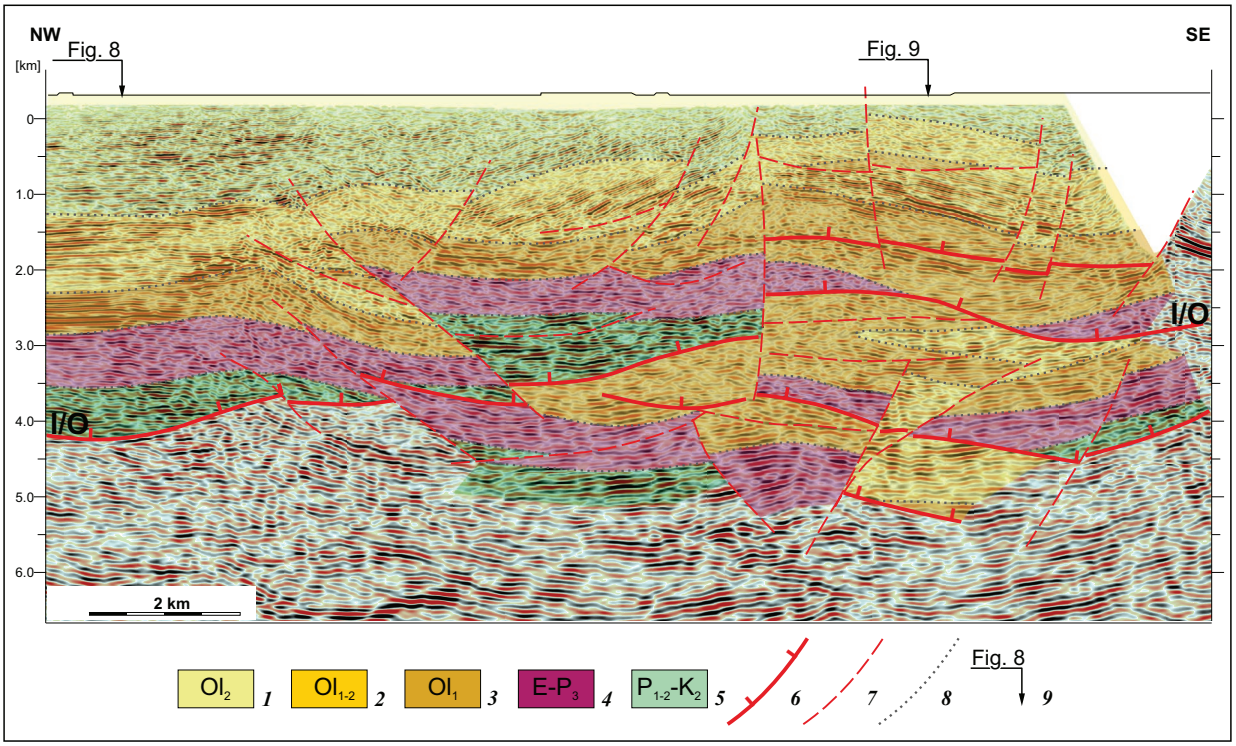

Fig. 10. Longitudinal cross-section through the western part of the Silesian Synclinorium (from Kuśmierek et al. 2019). Silesian Series: 1 – Upper Krosno Beds; 2 – Lower Krosno Beds; 3 – Menilite and Transitional beds (undivided); 4 – Hieroglyphic Beds, Variegated shales, and Ciężkowice Sandstones (undivided); 5 – Istebna Beds; 6 – folds overthrusts, I/O – thrust of inner (southern) zone of the Silesian Synclinorium over its outer zone; 7 – second-order duplexes (decollements) and faults; 8 – lithostratigraphic boundaries; 9 – location of longitudinal cross-sections.

The peculiar tectonic style of the outer zone of the Silesian Synclinorium is best-illustrated by the geological-seismic cross-section located in its southern part (Fig. 11), which includes the deep N-1 well. This zone is contoured from the south by the Mokre Fold overthrust (I/O), from the north by the Silesian Nappe overthrust, and from the west by the Subsilesian Nappe overthrust, the latter disappearing in the border zone with the Ukrainian Carpathians. In that border zone, the Silesian and Skole synclinoria merge into the CDOC beneath the thick cover of the Krosno Beds (Fig. 2). The N-1 well profile reveals that the southern part of the outer zone of the Silesian Synclinorium is filled with the thick succession of the Krosno Beds, whose bottom surface had not been reached by the N-1 well, with its final depth being 4505 m.

The most intensively folded is the near-surface zone illustrated by the cross-section in Fig. 11, where steep, asymmetric, locally back-overturned folds are detached from the older, Cretaceous and Paleogene formations. These detachments, which have been identified for the first time on reprocessed seismic profiles (Kuśmierek 2010), show the geometry of flat arcs. They displace backwards (to the south) traces of imbricated overthrusts, thereby compensating for the amount of tectonic reduction of deep-seated formations, which were subjected to more advanced diagenesis and were thus less susceptible to folding (Fig. 11). This type of inversion tectonics is associated with the margins of depocenters of synorogenic sediments known also from the southern part of the Silesian Synclinorium (Fig. 5). The depocenters are controlled by the zones of significant relative heights of consolidated basement relief (Fig. 6).

Skole Synclinorium

The above-presented remarks are valid also for the deep part of the Skole Synclinorium explored by the P-1 well down to a depth of 7210 m (Fig. 12).

Lithostratigraphy of the Skole formations differs from that of the Silesian–Subsilesian formations by the evolution of Cretaceous–Lower Paleogene lithofacies, which underlie synorogenic sediments of the Krosno lithofacies (Fig. 3). This lithofacies is laterally interfingered with the Subsilesian formations in the plunging zone of the Subsilesian uplift, as revealed by, among others, the deep J IG-1 well (Żytko 2004). Maximum thicknesses of the Menilite-Krosno formations are related to the central part of the Skole Synclinorium, where the bottom surface of these formations was found in the P-1 deep well at a depth of 5010 m.

The final geological reinterpretation of 21 geological-seismic profiles positioned between the San River valley and the Polish–Ukrainian state border demonstrates that the structure of the entire buried part of the Skole Synclinorium is dominated by monovergent, imbricated thrusts.

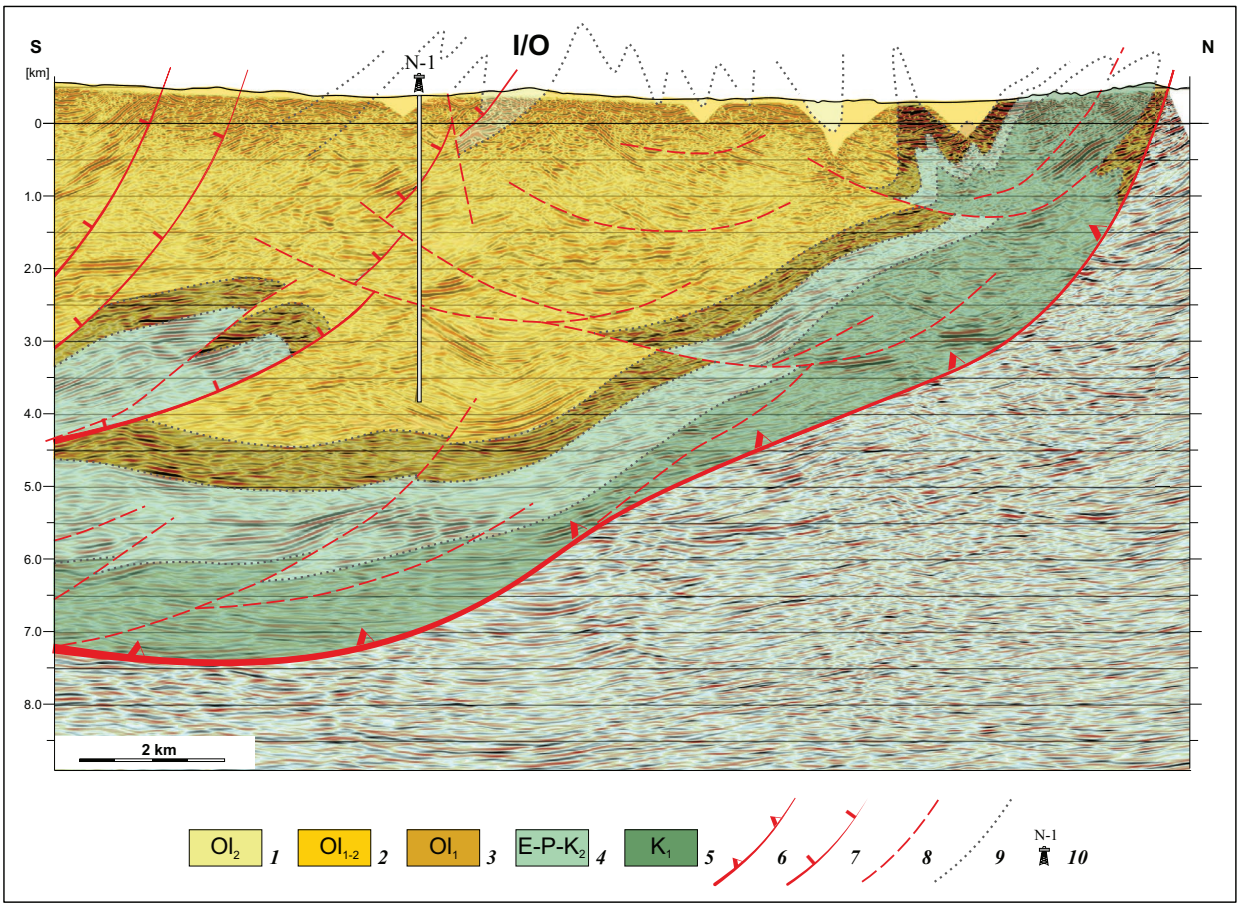

Fig. 11. Cross-section through the eastern part of the outer zone of the Silesian Synclinorium (from Kuśmierek et al. 2019). Silesian Series: 1 – Upper Krosno Beds; 2 – Lower Krosno Beds; 3 – Menilite and Transitional beds (undivided); 4 – Hieroglyphic Beds, Variegated shales, Ciężkowice Sandstone, Istebna Sandstone, and Godula Shale; 5 – Lgota, Wierzowa, and Cieszyn beds (undivided); 6 – overthrust nappes; 7 – folds overthrusts, I/O – the thrust of the inner (southern) zone of the Silesian Synclinorium over its outer zone; 8 – second-order duplexes (decollements) and faults; 9 – lithostratigraphic boundaries; 10 – well profile.

In the near-surface zone, these thrusts (locally backthrusts) show high dip angles and displace the hinges or limbs (mostly northern) of the folds (or, in fact, rather the duplexes), where complicated intersection patterns are seen on uncovered geological maps (e.g., Jasionowicz 1961; Gucik et al. 1980; Malata 1997).

The interpretation of seismic images of deeper zones in the Skole Synclinorium, reveals successive flattening of surfaces of the overthrusts associated with the evolution of second-order duplexes and flat decollements (Fig. 12), which do not appear on uncovered geological maps. Therefore, the true profiles of deep drillings commonly differ significantly from the expected ones, resulting in a variety of interpretations of deep geological structures (Kuśmierek et al. 2019).

Synthetic models of kinematic evolution of compressional sutures

Stratigraphic diversity of facies development and thicknesses of Upper Cretaceous–Cenozoic deposits, which constitute tectonostratigraphic units of the Middle Group (Fig. 3), is related to segmentation of the so-called Northern Basin (Książkiewicz 1972) into the Silesian and Skole subbasins by synsedimentary uplifts, contouring the depocenters of these subbasins (Fig. 2).

The inversion tectonics of older sedimentary formations compared with the younger cover of synorogenic sediments (Figs. 8–12) and, particularly, with the consolidated basement (Figs. 6, 7) emphasize the influence of time/space migration of tectonic movements as an explanation of complicated tectonic evolution of the Carpathian–Pannonian region (for details, see e.g., Khain et al. 1977; Książkiewicz et al. 1977; Jiříček 1979; Burchfiel & Royden 1982; Kuśmierek 1990, 1996; Konečný et al. 2002; Kuśmierek & Baran 2016).

Reconstruction of the inversion tectonics of synclinoria in the CDOC is supported by two reconstructed models, which determine the vertical component of tectonic movements in the epoch from the Upper Cretaceous to the Quaternary (Fig. 13) and the kinematics of tectonic movement rates during both the sedimentary and synorogenic stages (Fig. 14). Taking into account the reinterpreted results of magnetotelluric

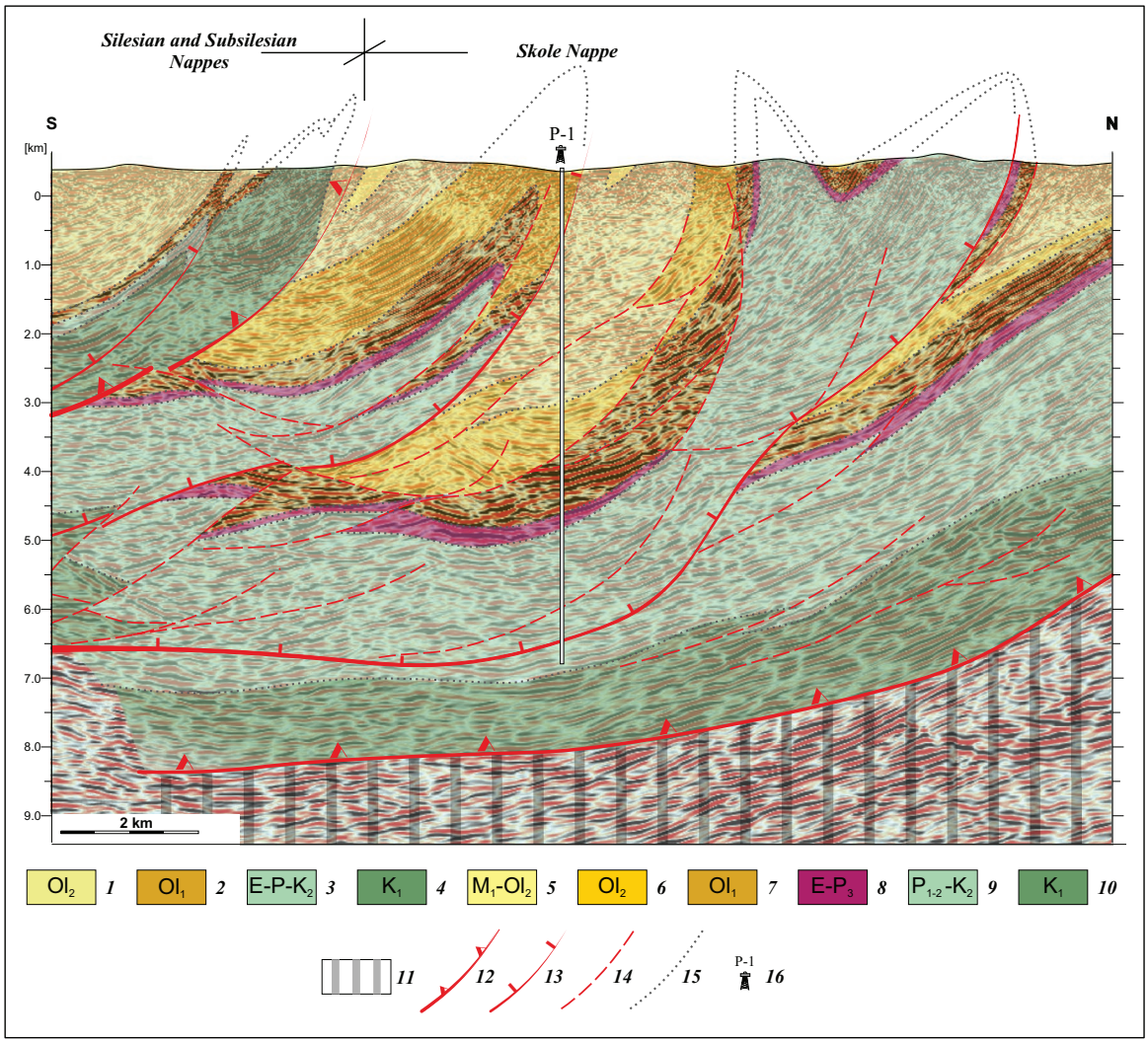

Fig. 12. Cross-section through the eastern part of the Skole Synclinorium (from Kuśmierek et al. 2019). Silesian and Subsilesian series: 1 – Krosno Beds (undivided); 2 – Menilite and Transitional beds (undivided); 3 – Variegated shales and Węglówka Marls; 4 – Lgota, Wierzowa, Grodziszcze, and Cieszyn beds (undivided). Skole Series: 5 – Upper Krosno Beds; 6 – Lower Krosno Beds; 7 – Menilite and Transitional beds (undivided); 8 – Hieroglyphic Beds and Variegated shales; 9 – Inoceramus Beds; 10 – Spas Shale and Spas Sandstone; 11 – unidentified stratigraphic formations resting upon the Precambrian basement; 12 – overthrust nappes; 13 – fold overthrusts; 14 – second-order duplexes (decollements) and faults; 15 – lithostratigraphic boundaries; 16 – well profile.

soundings and new geological-seismic cross-sections (Kuśmierek et al. 2019), these models better quantify the amounts of subsidence and convergence of sedimentary cover and its consolidated basement in comparison with earlier results (e.g., Kuśmierek 1990, 1996, 2010; Kuśmierek & Baran 2016).

Tectonic movements within the sedimentary cover between the Upper Cretaceous and Cenozoic

The trends of the vertical component of tectonic movements within the sedimentary cover were determined by subsidence hypsometric curves of the bottom surfaces of Senonian–Eocene and Oligocene–Lower Miocene formations (Fig. 13), assigned to averaged values of:

- chronostratigraphic horizons 33.9 and 16.0 Ma, which define geological time spans ascribed to distinguished stages of tectonic evolution, in fact, diachronously interfingered in the northeastern segment of the Outer Carpathians (from Kuśmierek & Baran 2016);
- deposition depth of the bottom of distinguished lithofacies, from the Upper Cretaceous to the Eocene (from Książkiewicz 1975), in the form of a bathymetric curve (B in Fig. 13);
- paleothicknesses of Senonian–Eocene and Oligocene–Lower Miocene formations determined from 16 and 65 profiles respectively (after Kuśmierek et al. 1991–1994).

The initial values of sediments paleothicknesses were reconstructed by summation of: (i) recent stratigraphic thicknesses (ms), (ii) increase of thicknesses resulting from tectonic deformations (Δm) due to (iii) reduction of the width of their

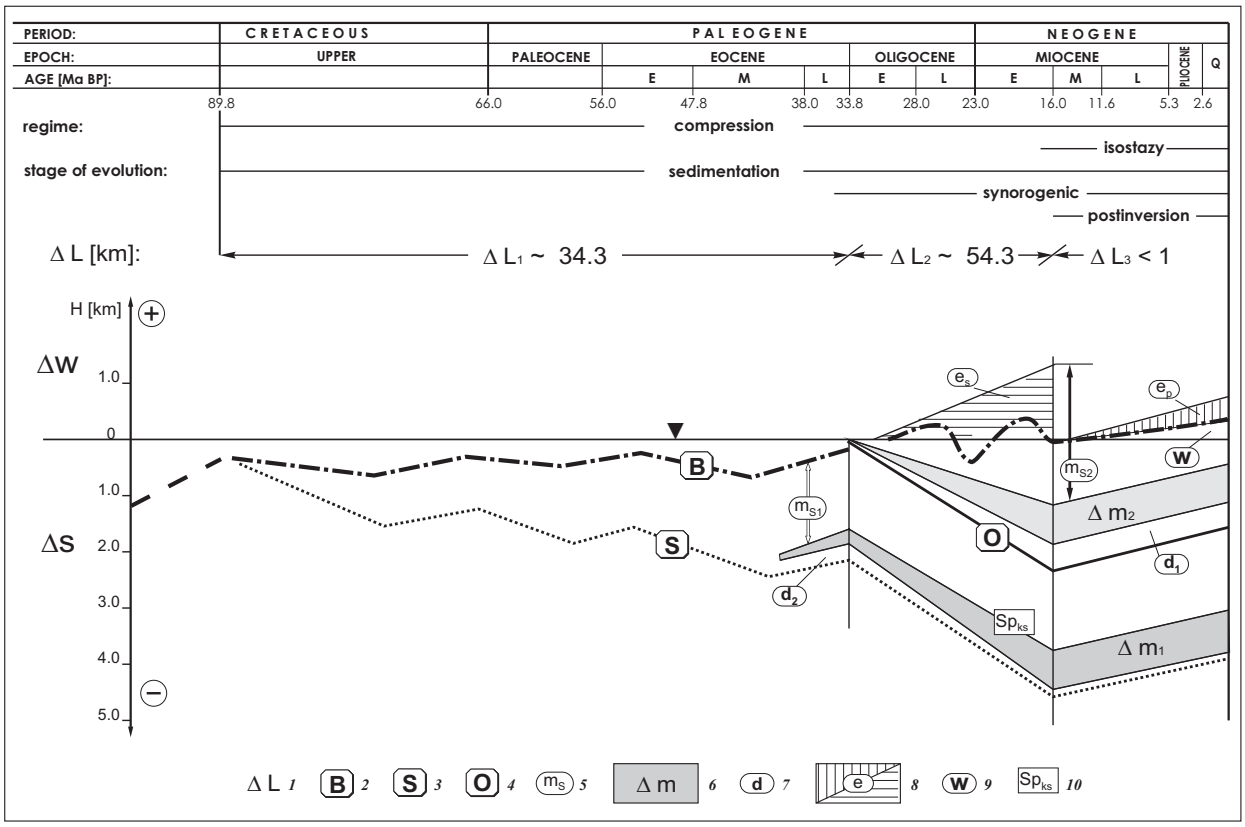

Fig. 13. Trends of the vertical component of tectonic movements within sedimentary cover during the Upper Cretaceous–Cenozoic period (averaged values). 1 – amounts of horizontal reduction of the width of sedimentation zones (tectonic convergence) in sedimentary cover: ΔL_1, ΔL_2, and ΔL_3 [km] during distinguished evolution stages of the CDOC referred to their ages (geological time scale from Ogg et al. 2016). Subsidence scale (ΔS): 2 – synthetic bathymetric curve B showing deposition depth of the bottom of distinguished Upper Cretaceous–Eocene lithofacies (from Książkiewicz 1975); 3 – subsidence of the bottom of Upper Cretaceous–Eocene formations (S); 4 – subsidence of the bottom of Oligocene–Lower Miocene formations (O; archival data, from Kuśmierek et al. 1991–1994); 5 – thicknesses of distinguished formations of sedimentary cover (m_{s1} – Upper Cretaceous–Eocene, m_{s2} – Oligocene–Lower Miocene); 6 – increase of thickness controlled by the amount of convergence (Δm_1, Δm_2); 7 – amount of compaction of clay lithofacies (d_1, d_2). Amount of uplift (ΔW): 8 – the amount of erosion during synorogenic (e_s) and post-inversion (e_p) stages; 9 – the amount of uplift (W); 10 – the bottom surface of Senonian sediments before compaction (Sp_{ks}).

deposition zones during the sedimentary stage (ΔL_1), and (iv) this reduction during the synorogenic stage (ΔL_2), and (v) densometric correction (Δd), which represents densification degree of clay lithofacies.

The value of width reduction (shortening) ΔL_2, which is 54.3 km (Fig. 13), was calculated as an average value of tectonic reduction from palinspastic models of No. III, IV, and V traverses positioned within the study area (Kuśmierek & Baran 2016, table 1). The ratio of ΔL_2 value to the number of subhorizontal movements of the basement obtained in the above-discussed models (ΔL_p=72.9 km) gave the value 0.74 of tectonic convergence coefficient. Considering the averaged amount of basement transport for the whole compressional regime calculated as 119 km (after Kuśmierek 1996; Kuśmierek et al. 2001), the value ΔL_1 calculated as (119.0–72.9)×0.74 equals 34.3 km.

The amount of subsidence (ΔS) was reduced:

- for the synorogenic stage, by the amount of uplift (ΔW) referred to the amount of synsedimentary erosion (e_s);
- for the post-sedimentary stage, by the amount of uplift of area morphology (related to the sea level datum) and by the amount of post-sedimentary erosion (e_p) (from Kuśmierek et al. 1995, 2001, Maćkowski et al. 2009).

The geometry of hypsometric curves illustrates strongly increasing subsidence in the synorogenic stage that corresponds to the number of subhorizontal displacements (ΔL_2 and ΔL_1) and documented by the highest deposition rate of the Krosno lithofacies (average value about 150 m/Ma; from Kuśmierek 1990), simultaneous with its tectonic deformation and erosion of synsedimentary uplifts.

Different subsidence trends of the bottom of the Oligocene formation in comparison with the bottom of the Senonian succession triggered the disharmonic tectonic style in the study area. Fading compression was accompanied by generally concordant uplift of both sedimentary covers during the post-inversion stage, controlled by isostasy and supported by the amount of erosion of uplifting tectogene (Kuśmierek 1990).

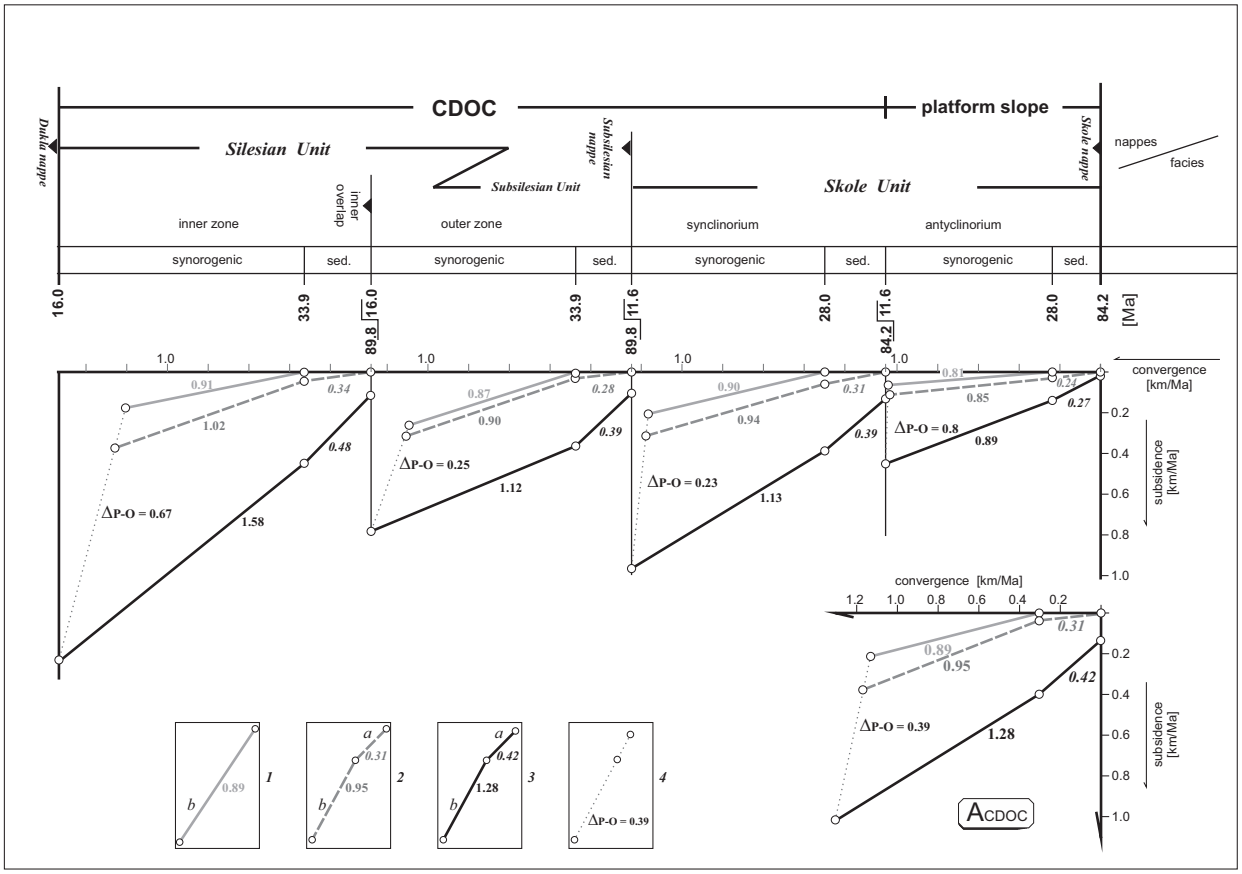

Fig. 14. Kinematic models of the rates of tectonic movements within the sedimentary cover and its consolidated basement. Diagrams of resultant rates of tectonic movements before Upper Miocene inversion controlled by the amounts of horizontal (convergence) and vertical (subsidence) displacements. Values of movement rates [km/Ma] for selected surfaces: 1 – bottom of Oligocene sediments during synorogenic stage (b); 2 – bottom of Senonian sediments during sedimentation (a) and synorogenic (b) stages; 3 – top of consolidated basement during sedimentation (a) and synorogenic (b) stages; 4 – difference ($\Delta_{P\text{-}O}$) between rates of tectonic movements of the bottom of Oligocene sediments O and the top of consolidated basement P. Particular diagrams were ascribed to distinguished nappes (facies), the CDOC structural elements and platform slope. Diagram A_{CDOC} illustrates averaged values for the CDOC, in comparison with the upper diagram representing values for platform slope.

Kinematic models of the rate of tectonic movements of sedimentary cover and its basement

Reconstruction of the rate of tectonic movements was based on the integration of the following elements:

- projection of recent and initial (precompressional) tectonics of the top of consolidated basement using the Radoszyce–Przemyśl magnetotelluric cross-section (Fig. 6);
- the results of palinspastic reconstruction of Oligocene–Lower Miocene sediments and their basement during the synorogenic stage (from No. V traverse of position similar to the line of magnetotelluric cross-section, table 1 in Kuśmierek & Baran 2016), supported by the total amount of basement displacement along that traverse in the Upper Cretaceous–Paleogene period (from Kuśmierek 1996, Figs. 5 and 6);
- averaged convergence and subsidence models ascribed to structural datum surfaces (P – top of the basement, S – bottom of Upper Cretaceous–Eocene formations and O – bottom of Oligocene–Lower Miocene formations) of distinguished structural elements in the CDOC and on the platform slope, as well as stages of their compressional evolution in geological periods (geological time scale from Ogg et al. 2016) and taking into account their propagation towards the Carpathian Foredeep (Fig. 14).

The kinematics of tectonic movements of the above-mentioned structural elements (zones) and structural surfaces is presented by synthetic diagrams of their resultant rates, which are controlled by:

- the amounts of convergence (horizontal displacement) and subsidence during the sedimentation stage (in fact, the sedimentation-tectonic, pre-orogenic stage) marked (v_1), and during the synorogenic stage, marked (v_2);
- the Δv_2 values, i.e. the difference between burial rates of datum surfaces: the top of the basement (P) and the bottom of Oligocene–Lower Miocene formations (O) during the synorogenic stage.

The element A_{CDOC} in Fig. 14 shows the averaged rate of tectonic movements within the structural elements of CDOC in comparison with the diagram of the Skole Nappe anticlinorium localised on the platform slope.

The rates of tectonic movements determined for the synorogenic stage are about 3 times higher than those obtained for the sedimentary-tectonic stage. This is particularly evident in diagrams representing the basement top surface in the inner zone of the Silesian Synclinorium, which was affected by the formation of longitudinal, sub-vertical, Type 2 compressional sutures. Amplitudes of these sutures depend on their throw values h_1–h_2 (Fig. 6) and the amount of uplift during the post-inversion stage, following the vertical component model of tectonic movements (Fig. 13).

For all diagrams, the amounts of horizontal displacements during both the sedimentation and the synorogenic stages were adjusted to the total convergence of the consolidated basement in the geological periods: 89.8–16.0 Ma for the Silesian Nappe (facies) and 84.2–11.6 Ma for the Skole Nappe (facies). These time spans correspond to deposition episodes of the Upper Cretaceous–Lower Miocene formations of the Silesian and the Skole facies before their tectonic inversion stage. It must be emphasized that small, horizontal displacements were neglected (for details, see Kuśmierek & Baran 2016, Fig. 10a). Within the geological periods mentioned above, for synorogenic sedimentary cover and its basement, different time spans were adopted for the Silesian facies: 33.9–16.0 Ma and for the Skole facies: 28.0–11.6 Ma (under the chronostratigraphic model in Fig. 3A). This provided a better fitting when compared to the model presented previously by Kuśmierek & Baran (2016, table 1).

According to Kuśmierek et al. (1991–1994), during the synorogenic stage, the amount of basement convergence within the range of the Silesian facies (i.e., Silesian and Subsilesian nappes, jointly) was 39.8 km and within the Skole facies, it was 29.2 km. The calculated tectonic convergence coefficient value of the basement for the frontal Skole overthrust was 0.15 during the synorogenic stage. This value was accepted as valid for the sedimentary–tectonic stage. For the convergence of synorogenic sedimentary cover (Silesian facies – 31.3 km and Skole facies – 28.3 km), this coefficient was about 0.05.

The amount of subsidence, which is the vertical component presented in the Sn and O diagrams (Fig. 14), was determined from the archival datasets (from Kuśmierek et al. 1991–1994) and integrated with the magnetotelluric cross-section (Fig. 6). Additionally, the averaged values of subsidence of distinguished structural elements were integrated as well, and determined from the intersections of overthrusts and corresponding, hypothetically-interpolated depths to the top of the consolidated basement (h_1–h_7) of: (i) Dukla Nappe (h_1), (ii) thrust of the inner zone of Silesian Synclinorium over the outer zone (h_2), (iii) thrust of the Subsilesian Nappe (h_3 and h_4), (iv) thrust of the Skole Nappe (h_5 and h_6), and (v) boundaries separating its synclinoria and anticlinoria (h_7; from Kuśmierek & Baran 2016, Fig. 10). Averaged subsidence values represented by initial stratigraphic thicknesses determined from burial depth maps for the preinversion stage (from Kuśmierek et al. 1991–1994, app. 9A, B, C, app. 25A, C) were adjusted to detailed chronostratigraphic intervals ascribed to deposition periods of the Silesian and the Skole facies (Fig. 14).

One important factor in the concept of inversion tectonics of the CDOC is the evident diversity of resultant rates of tectonic movements observed for the top of the consolidated basement and the bottom of the Oligocene sedimentary cover ($\Delta_{P\text{-}O}$) during the synorogenic stage. This is especially well-marked in the area between the CDOC and the platform slope (anticlinorium of the Skole Nappe). Within the CDOC, the difference among these resultant rates varies from 0.67 to 0.23 km/Ma (0.39 km/Ma, on average) and is much higher than the value for the platform slope: 0.08 km/Ma (Fig. 14 and $14A_{CDOC}$).

Scenario of inversion tectonic movements – a discussion

Regional geostructural background

The monovergent geometry of nappes thrusts overlapping the dislocated segments of the basement suggests a common scenario of their geodynamic evolution caused by diachronous subduction of the foreland platform (e.g., Bally 1975; Kuśmierek & Ney 1988; Konečný et al. 2002).

The southern range of subduction is contoured by 0-values of the geomagnetic induction vector (Fig. 1), which discloses the collision zone of the foreland platform with the lithosphere of the Internides (Jankowski et al. 1979). Depth to the platform top surface increases from 16 to 25 km east from the M-J deep fracture (Praus et al. 1981; Żytko 1999) and correlates with an abrupt reduction of crustal thickness on the northern slope of the Pannonian mantle diapir (Zeyen et al. 2002, profile V; Bezák et al. 2023).

The radial propagation of subduction advancing from the collision zone towards the flexural slope of the platform was controlled by segmentation of the platform basement, concordant with the northeastern trend of expansion of nappes overthrusts (see e.g. Jiříček 1979; Oszczypko & Ślączka 1985).

Considering the oroclinal shape of sedimentary basins associated with the pre-orogenic uplift of the Pannonian mantle diapir, the key factors influencing the diversity of evolution models of compression are transversal deep fractures, which rotated the basement segments (Doktór et al. 1990; Ryłko & Tomaś 2005). The presence of such deep fractures is revealed by discrepancy of nappes sheets and change of nappe-sheet tectonic style observed in the western part of the Polish Carpathians (where the platform slope is relatively shallow) into the nappe-fold style in the CDOC. Such style suggests vertical rotation of subduction zones in the younger Cenozoic, thus generating discontinuities in the sedimentary cover.

The subduction of the European Platform was driven by the expansion of both the Northern Atlantic and Arctic rifts (Książkiewicz et al. 1977). Its older sedimentary-tectonic stage (Upper Cretaceous–Eocene) revealed progressive segmentation

of a sedimentary basin into the subbasins of diverse facies development and thicknesses of coarse-detrital formations. The subbasins were bordered by synsedimentary uplifts triggered by the isostasy of doubled basement segments. During that stage, the essential structural discontinuity was formed, represented by subhorizontal decollements of sedimentary cover (i.e., in-sequence regional overthrusts) from the top surface of the consolidated basement, which gave rise to different styles of tectonic deformations (Kuśmierek 2010).

The recent tectonics of the Outer Carpathians was decisively influenced by the synorogenic stage of compression associated with the oroclinal migration of subduction and Neogene volcanics along the Carpathian arc (Burchfiel & Royden 1982; Konečný et al. 2002; Kuśmierek & Baran 2016). This model is typical of the northern branch of the European Alpide belt and supports the concept of subduction segmented by subparallel deep fractures (Ashgirey & Kropačev 1984; Roure et al. 1993; Kuśmierek et al. 2001).

Central Depression of the Outer Carpathians (western part)

The geological reinterpretation of magnetotelluric soundings recorded with the MT-1 system provides a new, detailed image of the consolidated basement (Figs. 6, 7) in comparison with the previous results (e.g., Stefaniuk 2003, 2006; Stefaniuk et al. 2009). This image enables researchers to compare the evolving basement structure with the compressional tectonics of: (i) tectono-erosional discontinuities at the bottom of flysch formations and (ii) the younger structural discontinuity at the bottom of the synorogenic sedimentary cover (Figs. 8–12), induced by isostatic rebound of subducted basement segments.

The western part of the CDOC is cut by two regional, transversal deep fractures: M-J and Ł-P already identified by palinspastic reconstruction of the compressional orogenic stage. At the beginning of this stage, the deposition range of epicontinental Skole subfacies had been greatly extended (by some tens of kilometres) in comparison with the recent position of the frontal overthrust of the Skole Nappe (Kuśmierek & Baran 2016, Figs. 8, 10).

The recent flexural platform slope is surrounded by deep basement depressions of the CDOC inherited after the synorogenic stage. Therefore, the basement is a complicated mosaic of tectonic blocks separated by faults (e.g., Doktór et al. 1990; Kuśmierek 2010), as demonstrated by the non-continuous intersection of the axes of gravity anomalies (Figs. 1, 6, 7).

Converging directions of longitudinal deep fractures (operating as compressional sutures having maximum amplitudes of displacements) and the strikes of nappes overthrusts (Fig. 7) suggest a common scenario of the geodynamic evolution of sedimentary covers and their basement; however, of strongly diverse geometry and kinematics of tectonic deformations.

The highest rate of tectonic movements was observed during the synorogenic stage, as indicated by the values of convergence and subsidence coefficients (Figs. 13, 14). It was driven by the vertical trend of movements of basement segments in the subduction zone. This trend was increasing from the platform slope towards the southern margin of CDOC, in the zone of collision with the lithosphere of the Internides where Neogene magmas were generated (Konečný et al. 2002). This stage was also associated with the development of depocenters of synorogenic sedimentary cover (Figs. 2, 3, 6) and was combined with the burial of eroded-off, initial synsedimentary uplifts.

The reduction (narrowing) ratio of sedimentary cover in relation to its basement during the synorogenic stage, with an average value of 0.74, justifies the origin of structural discontinuity (IN) located at the bottom of the synorogenic sedimentary cover (Figs. 8–12).

The inversion of the CDOC tectonics was undoubtedly directly influenced by deep fractures, which controlled the rotation and/or the directions of movements of the consolidated basement marked in Fig. 7, e.g.:

- the Y1 deep fracture, which shortened the width of the inner zone of the Silesian Synclinorium and triggered the development of numerous duplexes, not found on the northwestern part of the longitudinal cross-section (Fig. 10);
- the oblique-slip Ł-P deep fracture (Figs. 6, 7), whose origins in the zone of frontal overthrust is related to the Przemyśl Sigmoid (Kuśmierek 2010; Kuśmierek & Baran 2016). In the southern part of the CDOC, this deep fracture shows transpressive nature and duplicates the segments of the consolidated basement (Fig. 5) In the eastern part of the CDOC, the Ł-P fracture is accompanied by several second-order faults (marked X_1, X_{2-3} and X_4, in Fig. 7), whose contour disharmonic folds within Cretaceous–Paleogene formations and backthrows in the foreland of the Dukla Nappe (Fig. 5), (Kuśmierek 1979, 2010).

The presence of backthrusts, which is typical of the southern margin of the CDOC, indicates the advanced compression during the synorogenic stage and is reflected by the reconstructed amount of synsedimentary erosion (Fig. 13) and diverse morphology of the study area (Kuśmierek 1990; Kuśmierek et al. 2001).

Summary

- Reinterpretation of the new geophysical images provides detailed geometry of the inversion tectonics of the CDOC, previously concluded only from the profiles of deep wells.
- Inversion tectonic structures disclosed by deep cross-section are contoured by surfaces of tectonic and erosional discontinuities, deep-seated faults, nappes and out-of-sequence thrusts, second-order duplexes, and local backthrusts.
- The oldest tectonic discontinuities are transversal, oblique-slip deep fractures, which rotated the segments of the consolidated basement and were still active in the Neogene. Their initial evolution might have been related to the pre-compressional stage of expansion of sedimentary basins.

- The younger, subhorizontal, in-sequence thrusts were generated by decollements of flysch sediments susceptible to deformations (mostly Cretaceous clayey rocks) from the tectonic-erosional top surface of the consolidated basement (less commonly from the younger, thick-bedded sandstone formations). This process was synchronous with the propagation of subduction towards the foreland associated with the consumption of the foreland in the areas of inner synsedimentary uplifts.
- Accommodation of the initial width of the subducted foreland platform was intensified during the synorogenic stage, due to vertical rotation of platform segments cut by the youngest generation of vertical, longitudinal deep fractures. During that stage, the younger structural discontinuity was generated at the bottom of the synorogenic sedimentary cover.
- Convergent directions of sub-vertical deep fractures and intersections of thrusts (as well as the axes of minimum gravity anomalies), along with discrepancy of sedimentary nappes superimposed on the zones of regional transversal fractures, all suggest a common scenario of geodynamic evolution of sedimentary covers and their basement, which is in contrast to the hypothesized thin-skinned tectonics of the Outer Carpathians.
- The credibility of the interpretation of new geological and geophysical images of CDOC inversion tectonics is supported by kinematic models generated from separate archival datasets.

Acknowledgements: Both the models and the cross-sections presented above were based upon the results of research projects commissioned by the Polish Oil and Gas Co. in the years 1998–2000, 2013 and 2014, and upon grant No. BG2/ShaleCarp/14 financed by the National Centre for Research and Development. This project was partly funded by the funds (16.16.140.315) of the Faculty of Geology, Geophysics and Environmental Protection, AGH – University of Krakow. The authors thank anonymous reviewers for valuable comments and suggestions that have improved the quality of our publication

References

Ashgirey G.D. & Kropačev S.M. 1984: Tektoničeskaja subdukcja. In: Geologia Sovetskich Karpat. Kiev, 3–11 (in Russian).

Bally A.W. 1975: A geodynamic scenario for hydrocarbon occurrences. In: 9th World Petroleum Congress Proceedings, vol. 2, 33–44.

Baran U. & Jawor E. 2009: Seismogeologic documentation of prospects for new gas discoveries in Miocene sandstones under the Carpathian overthrust between Husów and Przemyśl. *Geologia – Kwartalnik AGH* 35, 223–253 (in Polish with English summary).

Bezák V., Bielik M., Marko F., Zahorec P., Pašteka R., Vozár J. & Papčo J. 2023: Geological and tectonic interpretation of the new Bouguer gravity anomaly map of Slovakia. *Geologica Carpathica* 74, 109–122. https://doi.org/10.31577/GeolCarp.2023.08

Burchfiel B.C. & Royden L. 1982: Carpathian Foreland Fold and Thrust Belt and its relation to Pannonian and other Basins. *AAPG Bulletin* 66, 1179–1195.

Czerwińska B. 2013: The present state of recognition of the study area. In: Górecki W. (Ed.): Geothermal Atlas of the Eastern Carpathians. Flysh Formations and Miocene/Mesozoic/Paleozoic Basement of the Polish Eastern Carpathians. Kraków, 121–127 (in Polish with English summary).

Czerwiński T. & Stefaniuk M. 2005: Magnetotelluric survey in the Carpathians – summary. *Biuletyn informacyjny PBG* 1, 57–65.

Doktór S., Graniczny M., Kucharski R., Mołek M. & Dąbrowska B. 1990: Subsurface geological structure of the Carpathians in the light of complex remote-sensing and geophysical analyses. *Przegląd Geol*ogiczny 11, 469–475 (in Polish with English summary).

Ďurkovič T., Koráb T. & Rudinec R. 1982: Deep structural borehole Zboj-1. *Regionálna Geológia Západných Karpát* 16, 6–76.

Gągała Ł., Vergés J., Saura E., Malata T., Ringenbach J.C., Werner P. & Krzywiec P. 2012: Architecture and orogenic evolution of the northeastern Outer Carpathians from cross-section balancing and forward modeling. *Tectonophysics* 532–535, 223–241. https://doi.org/10.1016/j.tecto.2012.02.014

Gucik S., Paul Z., Ślączka A. & Żytko K. 1980: Mapa geologiczna Polski w skali 1:200 000. Arkusz Przemyśl – Kalników, mapa bez utworów czwartorzędowych – wydanie B. *Instytut Geologiczny*, Warszawa (in Polish).

Jankowski J., Petr V., Pecová J. & Praus O. 1979: Induction vector estimates in the Polish–Czechoslovak part of the Carpathians. *Studia Geophysica et Geodetica* 23, 89–93.

Jankowski J., Petr V., Pecová J. & Praus O. 1984: Geoelectric anomaly in the Czechoslovak–Polish section of the Carpathians on the basis of geomagnetic and magnetotelluric sounding. *Acta Geodaetica, Geophysica et Montanistica Hungarica* 19, 81–91.

Jasionowicz J. 1961: O możliwości występowania ropy naftowej w północnym skrzydle fałdu Wańkowej wsi – Łodyny w okolicy Romanowej Woli i Serednicy (ark. Ustrzyki Dolne). *Biuletyn Instytutu Geologicznego* 166, 5–12 (in Polish).

Jiříček R. 1979: Tectonic Development of the Carpathian Arc in the Oligocene and Neogene. In: Maheľ et al.: Tectonic profiles through the West Carpathians. *GÚDŠ,* Bratislava, 205–214.

Jucha S. 1969: Jasło shales, their importance for stratigraphy and sedimentology of the Menilite-Krosno series. *Prace Geologiczne PAN* 52, 1–128 (in Polish with Russian and French summaries).

Jucha S. & Kotlarczyk J. 1958: Trial of new stratigraphics division of Menilite Series and Krosno Beds. *Nafta* 8, 205–207 (in Polish).

Khain V.J., Bjeer M.A., Byzowa S.L., Lomize M.G. & Rudakov S.G. 1977: Main features of the tectonic history of the Carpathians. *Vestnik Moskov. Univ. Geol.* 3, 3–20 (in Russian).

Klecker R., Bentham P., Palmer-Koleman S. & Jaminski J. 2001: A recent petroleum-geologic evaluation of the Central Carpathian Depression, Southeastern Poland. *Marine and Petroleum Geology* 18, 65–85. https://doi.org/10.1016/S0264-8172(00)00044-1

Kolodij V.V., Bojko G.Û. & Bojčevs'ka L.E. (eds.) 2004: Carpathian petroleum province. *The Ukrainian Publishing Center*, Lvov-Kiev, 1–387 (in Ukrainian with English summary).

Konečný V., Kováč M., Lexa J. & Šefara J. 2002: Carpatho-Pannonian region: an interplay of subduction and back-arc diapiric uprise in the mantle. *EGS Stephan Mueller Special Publication Series* 1, 165–195.

Kozikowski H. 1958: Geology of the Central Carpathian Depression between Żmigród and Sanok – The Polish Flysch Carpathinas. *Acta Geologica Polonica* 8, 471–500 (in Polish).

Książkiewicz M. 1956: Geology of the Northern Carpathians. *Geologische Rundschau* 45, 369–411.

Książkiewicz M. 1972: Geology of Poland. Vol. IV, Tectonics, part 3, Carpathians. *Wydawnictwa Geologiczne*, Warszawa, 1–228 (in Polish).

Książkiewicz M. 1975: Bathymetry of the Carpathian Flysch Basin. *Acta Geologica Polonica* 25, 309–367 (in Polish).

Książkiewicz M., Oberc J. & Pożaryski W. 1977: Geology of Poland, vol. IV, Tectonics. *Wydawnictwa Geologiczne*, Warszawa, 476–671 (in Polish with English summary).

Kuśmierek J. 1979: Gravitational deformations and backward overthrusts with references to deep structures and petroleum prospects of the Dukla unit foreland in the Bieszczady Mountains. *Prace Geologiczne PAN* 114, 1–68 (in Polish with English summary).

Kuśmierek J. 1981: Paleostructural analysis of the Otryt Series (southeast part of the Central-Carpathian Depression). *Zeszyty Naukowe AGH, Geologia* 7, 97–116 (in Polish).

Kuśmierek J. 1990: Outline of geodynamics of Central Carpathian Oil Basin. *Prace Geologiczne PAN* 135, 1–85 (in Polish with English summary).

Kuśmierek J. 1996: Evolution of the Central Carpathian Oil Basin – quantitative interpretation. In: Roure F., Ellouz N., Shein V.S. & Skvortsov I. (eds): Geodynamic evolution of sedimentary basins. International Symposium Moscow, 1992. *Éditions Technip*, 281–303.

Kuśmierek J. 2010: Subsurface structure and tectonic style of the NE Outer Carpathians (Poland) on the basis of integrated 2D interpretation of geological and geophysical images. *Geologica Carpathica* 61, 71–85.

Kuśmierek J. & Baran U. 2008: Subsurface structure of the Carpathians in the zone of the Przemyśl Sigmoid: interpretation of seismic sections and assessment of hydrocarbon prospects. *Geologia – Kwartalnik AGH* 34, 365–384 (in Polish with English summary).

Kuśmierek J. & Baran U. 2013: Tectonic and geological characteristic of the eastern part of the Polish Carpathians and transborder zone with Ukraine; A. Eastern part of the Polish Carpathians. In: Górecki W. (Ed.): Geothermal Atlas of the Eastern Carpathians. Flysh Formations and Miocene/Mesozoic/Paleozoic Basement of the Polish Eastern Carpathians. Kraków, 52–68 and 74–82 (in Polish with English summary).

Kuśmierek J. & Baran U. 2016: Structure and tectonic evolution of the NE segment of the Polish-Ukrainian Carpathians during the Late Cenozoic: subsurface cross-sections and palinspastic models. *Geologica Carpathica* 67, 347–370.

Kuśmierek J. & Ney R. 1988: Problems of tectonics of the basement and development of structures of the cover in the eastern part of the Polish Carpathians. *Przegląd Geologiczny* 6, 318–325 (in Polish with English summary).

Kuśmierek J., Stefaniuk M. & Patyk B. 1985: Interpretacja stylu deformacji tektonicznych w przekrojach wschodniej części Karpat z wykorzystaniem elementów statystyki . *Nafta* 11–12, 333–341 (in Polish).

Kuśmierek J., Halat Z., Maćkowski T. & Papiernik B. 1991–1994: Balance of hydrocarbon resources in the Central Carpathian Basin. *Research project no. 9 0427 91 01, financed by KBN*, Warszawa, 1–105 (unpublished materials in Polish).

Kuśmierek J., Halat Z., Maćkowski T. & Papiernik B. 1995: Evolution and hydrocarbon potential of the Polish Carpathians. Integrated modelling interpretation in petroleum system of eastern part of allochthonous units. *Prace Geologiczne PAN* 138, 1–92 (in Polish with English summary).

Kuśmierek J., Migas J. & Mruk J. 2001: Geodynamiczna charakterystyka karpackiej formacji ropogazonośnej. *Polish Journal of Mineral Resources* 3, 151–166 (in Polish).

Kuśmierek J., Machowski G. & Maćkowski T. 2010: Seismogeological interpretation of the tectonics of Carpathian oil- and gas-bearing structures (examples from the Jasło-Krosno area). *Prace Naukowe Instytutu Nafty i Gazu* 170, 567–572 (in Polish with English summary).

Kuśmierek J., Machowski G. & Baran U. 2016: Seismic imaging of the tectonic style of the Central Carpathian Synclinorium in the Krosno–Besko area. *Prace Naukowe Instytutu Nafty i Gazu Państwowego Instytutu Badawczego* 209, 513–518 (in Polish with English summary).

Kuśmierek J., Baran U. & Machowski G. 2019: Deep tectonics of the Central Carpathian Depression (SE Poland): examples of geological reinterpretation of magnetotelluric soundings and seismic profiles. In: Jarzyna J., Krakowska-Madejska P., Sowiżdżał A. (eds.): CAGG-AGH-2019 International Scientific Conference: "Challenges in Applied Geology and Geophysics: 100th anniversary of applied geology at AGH University of Science and Technology". 10–13 September 2019, Kraków. Book of abstracts, 213–214.

Maćkowski T., Kuśmierek J., Reicher B., Baran U., Kosakowski P., Łapinkiewicz A.P., Machowski G., Papiernik B., Szczygieł M., Zając A. & Zych I. 2009: Two-dimensional models of the organic-matter thermal transformation and hydrocarbon expulsion in the transfrontier zone of the Polish and Ukrainian Carpathians. *Geologia, Kwartalnik AGH* 35, 191–222 (in Polish with English summary).

Maheľ M. (Ed.) 1974: Tectonics of the Carpathian-Balkan regions: explanations to the tectonic map of the Carpathian-Balkan regions and their foreland. *Geological Institute of Dionýz Štúr*, Bratislava, 1–454.

Malata T. 1997: Tectonic style of the Węglówka zone of the Polish Eastern Carpathians and its relationship to the Carpathian basement. *Biuletyn Państwovegoo Institutu Geologicznego* 376, 43–59 (in Polish).

Marecik T., Pieniądz K. & Smolarski L. 2008: Metholodogy of seismic data processing in the Przemyśl Sigmoid – selected procedures. *Geologia, Kwartalnik AGH* 34, 527–540 (in Polish with English summary).

McClay K. 2011: Introduction to thrust fault-related folding. In: McClay K., Shaw J.H. & Suppe J. (eds.): Thrust fault-related folding. *AAPG Memoir* 94, 1–19.

Nemčok M., Krzywiec P., Wojtaszek M., Ludhová L., Klecker R.A., Sercombe W.J. & Coward M.P. 2006: Tertiary development of the Polish and eastern Slovak parts of the Carpathian accretionary wedge: insights from balanced cross-sections. *Geologica Carpathica* 57, 355–370.

Nemčok M. & Henk A. 2006: Oil in foreland sourced by thrustbelt: insights from numerical stress modeling and balancing in the West Carpathians. *Geological Society London Special Publications* 253, 415–428. https://doi.org/10.1144/GSL.SP.2006.253.01.22

Nowak J. 1927: Outline of tectonics of Poland. In: II Zjazd Słowiańskich Geografów i Etnografów w Polsce. Kraków, 1–160 (in Polish).

Ogg J.G., Ogg G.M. & Gradstein F.M. 2016: A Concise Geologic Time Scale. *Elsevier*, 1–234.

Oryński S., Jóźwiak W., Nowożyński K. & Klityński W. 2022: Comparison of 3D, 2D, and 1D Magnetotelluric Inversion Results on the Example of Data from Fore-Sudetic Monocline. *International Journal of Geophysics* 2022, 3400950. https://doi.org/10.1155/2022/3400950

Oszczypko N. 2004: The structural position and tectonosedimentary evolution of the Polish Outer Carpathians. *Przegląd Geologiczny* 52, 780–791.

Oszczypko N. & Ślączka A. 1985: An attempt to palinspastic reconstruction of Neogene basins in the Carpathian foredeep. *Annales Societatis Geologorum Poloniae* 55, 55–75.

Oszczypko N., Ślączka A. & Żytko K. 2008: Tectonic subdivision of Poland: Polish Outer Carpathians and their foredeep. *Przegląd Geol*ogiczny 56, 927–935 (in Polish with English summary).

Praus O., Pecová J., Petr V., Pec K., Hvoždara M., Červ V., Pek J. & Lastovickova M. 1981: Electronic induction and electrical conductivity in the Earth's body. In: Zátopek A. (Ed.): Geophysical syntheses in Czechoslovakia. *VEDA*, Bratislava, 297–316.

Roure F., Roca E. & Sassi W. 1993: The Neogene evolution of the outer Carpathian flysch units (Poland, Ukraine and Romania): kinematics of a foreland/fold-and-thrust belt system. *Sedimentary Geology* 86, 177–201.

Ryłko W. & Tomaś A. 1995: Morphology of the consolidated basement of the Polish Carpathians in the light of magnetotelluric data. *Kwartalnik Geologiczny* 39, 1–16.

Ryłko W. & Tomaś A. 2005: Basement structure below the West Carpathian – East Carpathian orogen junction (eastern Poland, north-eastern Slovakia and western Ukraine). *Geologica Carpathica* 56, 29–40.

Ślęzak K., Jóźwiak W., Nowożyński K. & Brasse H. 2016: 3-D Inversion of MT Data for Imaging Deformation Fronts in NW Poland. *Pure and Applied Geophysics* 173, 2423–2434. https://doi.org/10.1007/s00024-016-1275-2

Starzec K. 2016: Opracowanie powierzchniowej mapy geologicznej dla obszaru koncesji Sobniów-Kombornia-Rogi pod kątem identyfikacji elementów składowych procesów generowania, migracji i akumulacji węglowodorów. *GEOKRAK* Mapa geologiczna, skala 1: 50 000 (in Polish).

Stefaniuk M. 2003: Regional magnetotelluric investigations in the Polish Eastern Carpathians. *Geologia, Kwartalnik AGH* 29, 3–4, 131–168 (in Polish with English summary).

Stefaniuk M. 2006: Some results of a new magnetotelluric survey in the area of Polish Outer Carpathians. In: Golonka J. & Picha F.J. (eds.): The Carpathians and their foreland: Geology and hydrocarbon resources. *AAPG Memoir* 84, 503–512. https://doi.org/10.1306/985624M843081

Stefaniuk M. & Kuśmierek J. 1986: Interpretation of the basement roof of the eastern part of Polish Carpathians in the light of magnetotelluric survey and geological premises. *XXXI International Geophisical Symposium,* Gdańsk, 232–240.

Stefaniuk M., Ostrowski C., Targosz P. & Wojdyła M. 2009: Some problems of magnetotelluric and gravity structural investigations in the Polish Eastern Carpathians. *Geologia , Kwartalnik AGH* 35, 7–46 (in Polish with English summary).

Świderski B. 1933: Sur l'arc des Karpathes occidentales. *Eclogae Geologicae Helvetiae* 26, 111–130 (in French).

Świdziński H. 1958: Mapa Geologiczna Karpat Polskich (część wschodnia), 1:200 000. *Wydawnictwa Geologiczne*, Warszawa (in Polish).

Świdziński H. 1971: Tectonics of the Polish Flysch Carpathians. *Zeszyty Naukowe AGH*, *Geologia* 309*,* 7–20 (in Polish).

Święcicka-Pawliszyn J. & Pawliszyn J. 1978: Zastosowanie badań magnetotellurycznych do rozpoznania złożonych struktur geologicznych. *Biuletyn PBG* 2, 16–25 (in Polish).

Tołwiński K. 1932: Affaisement central des Carpates. *Geol. Statystyka Naftowa*, Borysław 11, 362–366 (in French).

Tołwiński K. 1956: The chief tectonic elements of the Carpathian Mts. *Acta Geologica Polonica* VI, 75–226 (in Polish with English summary).

Wdowiarz S. 1985: Some problems of the geological structure and oil/gas productivity of the Central Carpathian Synclinorium in Poland. *Biuletyn Instytutu Geologicznego* 350, 5–45 (in Polish).

Woźnicki J. 1985: Low-resistivity element in the Carpathians. *Kwartalnik Geologiczny* 29, 153–166.

Żelaźniewicz A., Aleksandrowski P., Buła Z., Karnkowski P.H., Konon A., Oszczypko N., Ślączka A., Żaba J. & Żytko K. 2011: Tectonic subdivision of Poland. *Komitet Nauk Geologicznych PAN*, Wrocław, 1–60 (in Polish).

Zeyen H., Dérerová J. & Bielik M. 2002: Determination of the continental lithospheric thermal structure in the Western Carpathians: integrated modelling of surface heat flow, gravity anomalies and topography. *Physics of the Earth and Planetary Interiors* 134, 89–104. https://doi.org/10.1016/S0031-9201(02)00155-3

Żytko K. 1999: Korelacja głównych strukturalnych jednostek Karpat Zachodnich i Wschodnich. *Prace Państwowego Instytutu Geologicznego* 168, 135–164 (in Polish).

Żytko K. (ed.) 2004: Jasień IG-1. Profile głębokich otworów wiertniczych Państwowego Instytutu Geologicznego 103. *PIG*, Warszawa, 1–67 (in Polish).

Żytko K. (ed.) 2006: Brzegi Dolne IG-1. Profile głębokich otworów wiertniczych Państwowego Instytutu Geologicznego 107. *PIG*, Warszawa, 1–53 (in Polish).